Continental crust beneath southeast Iceland

Trond H. Torsvik[a,b,c,1], Hans E. F. Amundsen[d], Reidar G. Trønnes[a,e], Pavel V. Doubrovine[a], Carmen Gaina[a], Nick J. Kusznir[f], Bernhard Steinberger[a,g], Fernando Corfu[a,h], Lewis D. Ashwal[c], William L. Griffin[i], Stephanie C. Werner[a], and Bjørn Jamtveit[j]

[a]Centre for Earth Evolution and Dynamics, University of Oslo, N-0315 Oslo, Norway; [b]Geological Survey of Norway, Geodynamics, N-7491 Trondheim, Norway; [c]School of Geosciences, University of Witwatersrand, Wits 2050, South Africa; [d]Vestfonna Geophysical, N-8310 Kabelvåg, Norway; [e]Natural History Museum, University of Oslo, N-0318 Oslo, Norway, [f]Department of Earth and Ocean Sciences, University of Liverpool, Liverpool L69 3GP, United Kingdom; [g]Helmholtz Centre Potsdam, GeoForschungsZentrum, Section 2.5 Geodynamic Modelling, D-14473 Potsdam, Germany; [h]Geosciences, University of Oslo, N-0316 Oslo, Norway; [i]Core to Crust Fluid Systems/Geochemical Evolution and Metallogeny of Continents, Macquarie University, Sydney, NSW 2109, Australia; and [j]Physics of Geological Processes, University of Oslo, N-0316 Oslo, Norway

Edited by Norman H. Sleep, Stanford University, Stanford, CA, and approved March 11, 2015 (received for review December 4, 2014)

The magmatic activity (0–16 Ma) in Iceland is linked to a deep mantle plume that has been active for the past 62 My. Icelandic and northeast Atlantic basalts contain variable proportions of two enriched components, interpreted as recycled oceanic crust supplied by the plume, and subcontinental lithospheric mantle derived from the nearby continental margins. A restricted area in southeast Iceland—and especially the Öræfajökull volcano—is characterized by a unique enriched-mantle component (EM2-like) with elevated $^{87}Sr/^{86}Sr$ and $^{207}Pb/^{204}Pb$. Here, we demonstrate through modeling of Sr–Nd–Pb abundances and isotope ratios that the primitive Öræfajökull melts could have assimilated 2–6% of underlying continental crust before differentiating to more evolved melts. From inversion of gravity anomaly data (crustal thickness), analysis of regional magnetic data, and plate reconstructions, we propose that continental crust beneath southeast Iceland is part of ∼350-km-long and 70-km-wide extension of the Jan Mayen Microcontinent (JMM). The extended JMM was marginal to East Greenland but detached in the Early Eocene (between 52 and 47 Mya); by the Oligocene (27 Mya), all parts of the JMM permanently became part of the Eurasian plate following a westward ridge jump in the direction of the Iceland plume.

geology | continental crust | geochemistry | plumes | plate reconstructions

The North Atlantic Igneous Province covers vast areas in Baffin Island, Greenland, United Kingdom, Ireland, the Faroe Islands, and offshore regions (Fig. 1). Volcanic activity commenced ∼62 Mya (1) and is attributed to the impingement of a mantle plume head on the lithosphere (2). Enriched and depleted geochemical signatures in the Paleogene to Recent basalts from Iceland reflect a combination of plume-derived and shallow asthenospheric material, representing a classic case of plume–ridge interaction. The volcanic products of the Iceland plume have signatures of recycled oceanic crust and primordial-like material with high $^3He/^4He$ ratios (up to 50 R_A, where R_A is the $^3He/^4He$ ratio of air), spanning a range of refractory to fertile compositions (3, 4). Additional shallow-level contributions include the depleted mid-ocean ridge basalt–type asthenosphere, variably mixed with subcontinental lithospheric mantle material (5–8). The proximity of Iceland to the Jan Mayen Microcontinent (JMM) (Fig. 1) raises the question of whether Iceland includes underlying fragments of continental crust (9, 10). There are unconfirmed reports of both Precambrian and Mesozoic zircons in young basalts from Iceland, but only in abstract form (9, 11). The recovery of a 1.8-Ga-old grain from the most primitive Öræfajökull basalts (9) in southeast Iceland (Figs. 1 and 2*A*) is potentially very interesting, although two Jurassic zircon grains (160 Ma) uncovered in the same separation are now suspected to be due to laboratory contamination.

Evidence for Assimilation of Underlying Continental Crust in Southeast Iceland

In comparison with other Icelandic and northeast Atlantic rocks, the entire Öræfajökull rock suite, ranging from basalts to rhyolites, is characterized by high $^{87}Sr/^{86}Sr$, intermediate $^{206}Pb/^{204}Pb$, as well as $^{207}Pb/^{204}Pb$ and $^{208}Pb/^{204}Pb$ ratios that lie well above the Northern Hemisphere Reference Line (12) (Figs. 3 and 4). These geochemical features, which also include uniformly high $\delta^{18}O_{bulk\text{-}rock}$ of 4.8–5.9‰, have been attributed to an enriched-mantle (EM)-like mantle source (8, 13–15). We suggest here that the unique geochemical signature is caused by contamination of primitive basaltic melts with continental crust. Our modeling of the Sr–Nd–Pb abundances and isotope ratios demonstrate that the Öræfajökull basalts could be derived from basaltic rift-zone magmas similar to those in the Mid-Icelandic Belt by assimilation of 2–6% of continental crust (Fig. 5). The basalts of the Eastern Rift Zone and the Snæfell volcano (Fig. 2*A*) are compositionally intermediate between the Mid-Icelandic Belt and Öræfajökull basalts, indicating 0–2% and 2–6% assimilation of continental crust within the Eastern Rift Zone and Eastern Flank Zone, respectively (Figs. 3 and 5). This geographically restricted isotope array (Fig. 3) is unique in Iceland and the northeast Atlantic. It may possibly support the arrival of distinct and volumetrically limited enriched mantle material, e.g., recycled terrigenous sediments as an EM2-component (16) in the shallow melting zone of the plume. However, we favor a model with in situ continental crust contamination, and interpret the uniform O-isotope composition across the entire spectrum from basalt to rhyolite in the flank-zone volcanoes as indicating that the intermediate and silicic magmas were chiefly generated by fractional crystallization (17, 18). Assimilation of continental crust probably occurred at a deep level before the differentiation to evolved magmas, and we suggest that the source of continental material beneath southeast Iceland is a sliver of the JMM.

Significance

The Iceland hotspot is widely thought to be the surface expression of a deep mantle plume from the core–mantle boundary that can be traced back in time at least 62 My. However, some lavas contain continental material, which has previously been proposed to have been recycled through the plume. Here, we argue that the plume split off a sliver of continent from Greenland in the Early Eocene. This sliver is now located beneath southeast Iceland where it locally contaminates some of the plume-derived magmas.

Author contributions: T.H.T. and H.E.F.A. designed research; T.H.T., H.E.F.A., R.G.T., and C.G. performed research; T.H.T., H.E.F.A., R.G.T., C.G., and N.J.K. contributed new reagents/analytic tools; T.H.T., H.E.F.A., R.G.T., P.V.D., C.G., N.J.K., B.S., F.C., L.D.A., W.L.G., S.C.W., and B.J. analyzed data; and T.H.T., H.E.F.A., R.G.T., P.V.D., C.G., N.J.K., B.S., F.C., L.D.A., W.L.G., S.C.W., and B.J. wrote the paper.

The authors declare no conflict of interest.

This article is a PNAS Direct Submission.

Freely available online through the PNAS open access option.

[1]To whom correspondence should be addressed. Email: t.h.torsvik@geo.uio.no.

This article contains supporting information online at www.pnas.org/lookup/suppl/doi:10.1073/pnas.1423099112/-/DCSupplemental.

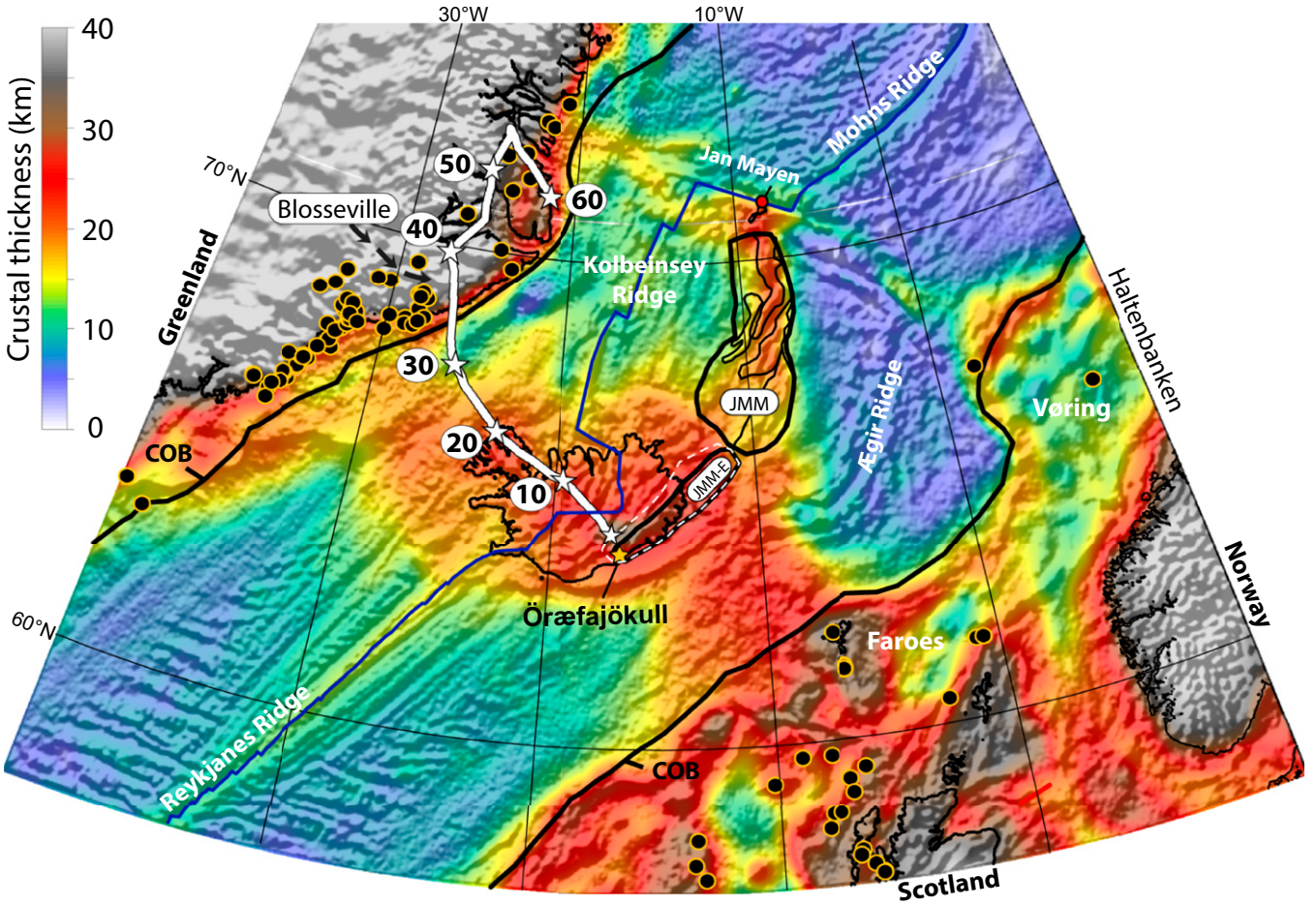

Fig. 1. Crustal thickness map based on gravity inversion and revised location of the Iceland plume (white star symbols in 10-My intervals) relative to Greenland back to 60 Ma (see Fig. 6*A* for details). Transition between continental and oceanic crust (COB, black lines), plate boundaries (blue lines), site locations for dated North Atlantic Igneous Province magmatism (yellow circles with black fill), and the estimated size of the "classic" Jan Mayen Microcontinent (JMM) and the extended JMM (JMM-E) are also shown. The classic JMM is ~500 km long (200 km at its widest and shown with four continental basement ridges), and crustal thicknesses are about 18–20 km (scale at *Upper Left*), which suggests considerable continental stretching before drifting off Greenland. We extend JMM 350 km southwestward (~70 km wide) beneath southeast Iceland where we calculate maximum crustal thicknesses of ~32 km (Fig. 2*B*). The size of JMM-E is a conservative estimate and could be as large as the white-stippled area. Öræfajökull location is shown as a yellow star.

Geochemical Modeling

The Sr–Nd–Pb isotope composition of Öræfajökull volcano has been interpreted to fall on a trend from a depleted mantle composition toward an enriched-mantle component, interpreted as EM1- or EM2-like (8, 13–15). Fig. 3 shows that the Sr–Nd–Pb isotopic mixing trajectories from depleted tholeiites of the Mid-Iceland Belt to the enriched Öræfajökull basalts largely point toward the EM2 component. One of the reasons that previous studies (13) have concluded that this unique isotope composition could be related to an EM-like mantle component is that the entire compositional range from basalts to rhyolites has uniform Sr–Nd–Pb isotope ratios, as well the uniform and rather high $\delta^{18}O_{SMOW}$ of 4.8–5.9‰ (Fig. 4). Anatectic contributions from a partially hydrated basaltic crust in Iceland would result in a strong decrease in $\delta^{18}O$ for evolved basalts and rhyolites in the volcanic rift zones, without affecting the long-lived radiogenic isotope systems appreciably (19). Minor assimilation of material from a Precambrian microcontinent rifted off from East Greenland, however, may appropriately elevate $^{87}Sr/^{86}Sr$, $^{207}Pb/^{204}Pb$, and $^{208}Pb/^{204}Pb$, relative to $^{143}Nd/^{144}Nd$ and $^{208}Pb/^{204}Pb$, to yield the observed isotopic arrays for the Öræfajökull rocks. The Öræfajökull composition could have been generated by direct contamination of primitive basaltic melts with in situ continental crust buried under southeast Iceland. The proposed Continental Crustal Contamination Trend (CCCT) (Fig. 3) differs from the other trends involving mantle source mixing and progressive melting in Iceland, and along the northeast Atlantic and Arctic spreading ridges (Fig. S1).

Sr–Pb–Nd isotope arrays (Fig. 3), including basalts from Iceland, Spitsbergen and the Reykjanes, Kolbeinsey (west of Spitsbergen), and Gakkel (High Arctic) Ridges, demonstrate that the CCCT is—unique and geographically limited—extending from the Mid-Iceland Belt via the Eastern Rift Zone and the Snæfell central volcano to the Öræfajökull central volcano. More extensive data for the entire northeast Atlantic and Arctic are presented by Trønnes et al. (20). Based on the observed CCCT, we modeled the Sr–Pb–Nd isotopic evolution of southeast Iceland using a range of continental crustal compositions (Fig. 5). Based on the prebreak location of the JMM, Precambrian rock compositions from the east Greenland coast were tested as contaminants. Whereas the crustal units of Blosseville Kyst (21, 22) in East Greenland (Fig. 1) have too unradiogenic Pb isotopes to match the southeast Iceland CCCT, the contamination trend defined by the upper series lavas in the Hold with Hope area further north provides a contaminant with acceptable isotope ratios (23). The gray bands in Fig. 5 represent mixing

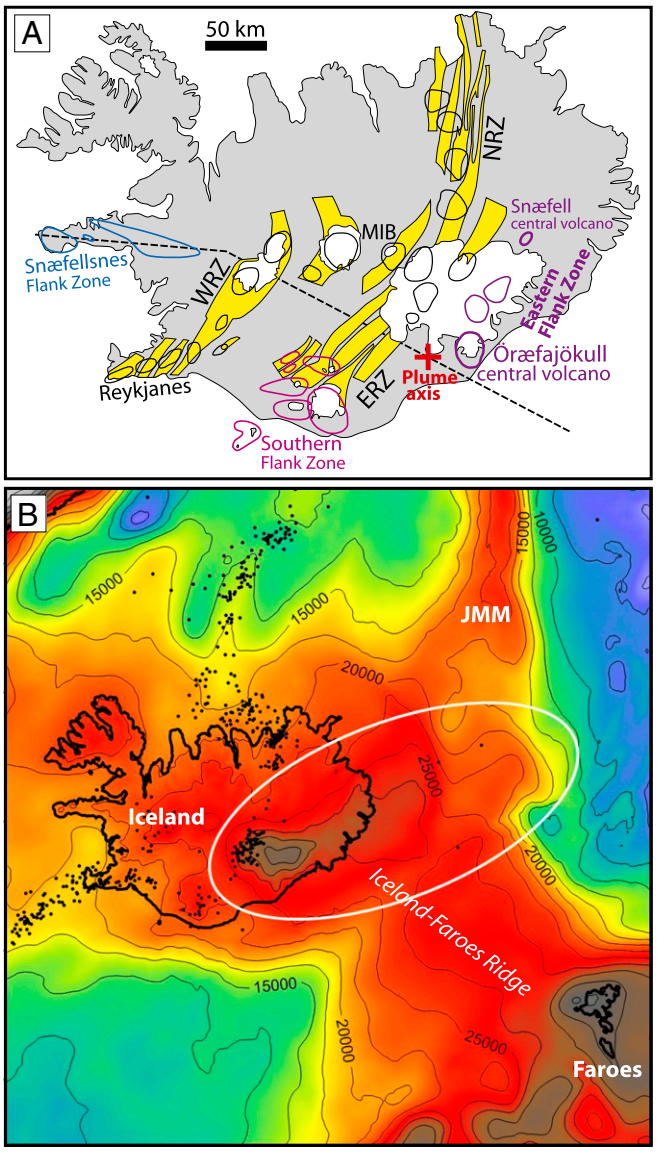

Fig. 2. (*A*) Simplified geological map of Iceland outlining the major rift zones (RZ), rift zone central volcanoes (black outline), flank zone central volcanoes (colored outlines), the location of the Öræfajökull central volcano, and the position of the current plume axis of Shorttle et al. (25). Yellow areas are fissure swarms. WRZ, ERZ, NRZ, and MIB: Western, Eastern, and Northern Rift Zone and Mid-Iceland Belt, respectively. The stippled west-northwest–trending line through the plume axis depicts the position of the cross sections in Fig. 9. (*B*) Enlarged crustal thickness map (Fig. 1) with superimposed earthquake locations (earthquake.usgs.gov/earthquakes) and contour intervals (in meters) showing that the anomalously thick crust under southeast Iceland extends offshore to the northeast suggesting that it is a southerly fragment of the Jan Mayen Microcontinent (JMM) rather than an extension of the southeast-northwest–orientated Iceland-Faroes Ridge.

lines between the average Mid-Iceland Belt composition and the Hold with Hope isotope ratio component, combined with Sr–Nd–Pb concentrations for the upper and lower continental crust models (24). An average of Haltenbanken sediment samples offshore central Norway (Dataset S1 and *Methods*), near the eastern conjugate margin of the JMM, is also an appropriate contaminant (thick red lines in Fig. 5). The wide ranges in Sr–Nd–Pb concentrations and isotopic ratios in the Precambrian crust of Greenland and Norway, however, cannot provide tight constraints on the crustal contaminant.

The CCCT can be modeled by incorporation of 2–6% of the continental crust components into basaltic melts similar to those erupted in the Mid-Iceland Belt to generate the Öræfajökull basalts (Fig. 3). The Snæfell basalts appear to record a corresponding contamination with 1–4% of continental crust. The Eastern Rift Zone basalts form a narrow sublinear array in the CCCT, with the sample localities furthest away from Öræfajökull showing no continental crust contamination, and those closest to Öræfajökull having 1–2% continental crust. A current plume axis position only about 35 km west of the Öræfajökull summit caldera (25) is consistent with mantle flow from a wider Öræfajökull region underlain by continental contaminants, toward Snæfell and across the Eastern Rift Zone toward the Mid-Iceland Belt.

Distribution of Continental Crust Beneath Southeast Iceland

Although the shape and size of the postulated fragment of continental crust residing beneath southeast Iceland is uncertain, we model it as a 350-km-long extended segment of the JMM (JMM-E in Fig. 1). This tectonic block was probably ~70 km wide according to our reconstructions of East Greenland and Eurasia near the breakup time (see Fig. 7*A*); JMM-E must fit between East Greenland and the Faroes (now part of Eurasia), assuming that there was no younger extension between the Faroes and Eurasia after breakup. The precise width also depends on identifying the exact transition between continental and oceanic lithosphere [continent–ocean boundary (COB)] in East Greenland and the conjugate margin offshore the Faroes (Fig. 6*A* and Fig. S2). The latter is reasonably defined, but the East Greenland COB interpretation is complicated by offshore seaward dipping reflectors (associated with the opening of the northeast Atlantic) and the younger Iceland–Greenland volcanic ridge.

The JMM structure has been divided into several distinct segments based on potential field and seismic data (26–28). The original size of these blocks was smaller than at present, and the fact that they are now composed of extended continental crust is also reflected in the estimation of shallow Moho depths (18–20 km) from gravity inversion (Figs. 1 and 2*B*). The gravity inversion—which incorporates a lithospheric thermal gravity-anomaly correction (refs. 29 and 30; *Methods*)—predicts that the thicker crust of the JMM, compared with that of the oceanic basins to the east and west, extends southwestward under south-east Iceland. Sensitivity tests (Fig. S3) show that the prediction of thick crust on the JMM and beneath southeast Iceland (up to 32 km; Fig. 2*B* and Fig. S4) is not significantly dependent on sediment thickness or preferred crustal density (2,850 kg·m^{-3}). Crustal thicknesses for the JMM and flanking ocean basins are consistent with seismic refraction

Table 1. Predicted location of the Iceland plume relative to the Greenland plate (Figs. 1, 6*A*, and 7) based on a global moving-hotspot reference frame (33)

Age, My	Latitude, °	Longitude, °
0	64.48	342.95
5	64.95	341.75
10	65.42	340.50
15	65.81	338.72
20	66.28	336.84
25	67.03	335.14
30	67.52	334.20
35	68.58	333.55
40	69.83	332.70
45	70.43	334.01
50	71.68	334.29
55	72.37	335.54
60	71.27	338.35

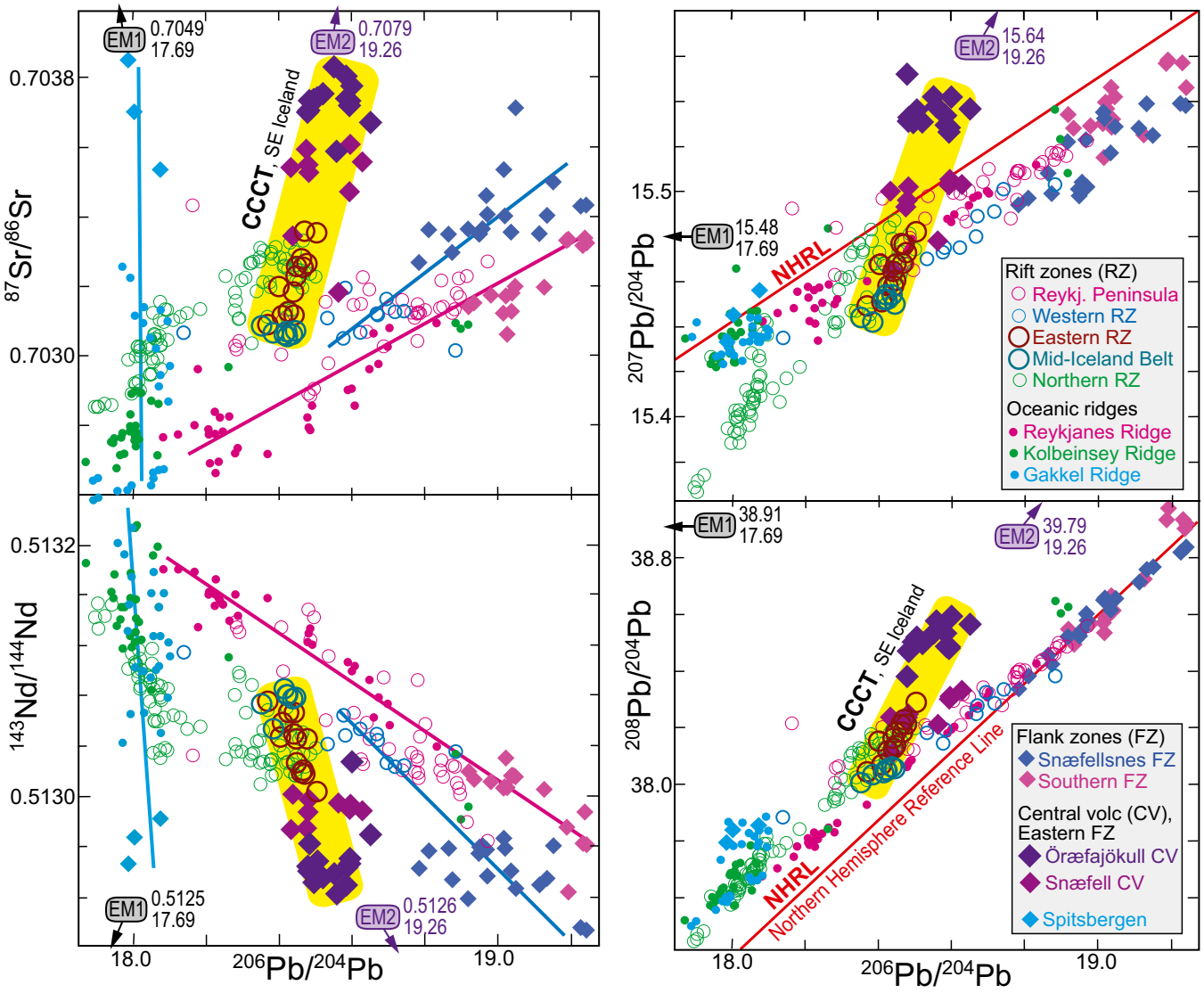

Fig. 3. The Sr–Nd–Pb isotopic composition of basalts from the Icelandic rift and off-rift (flank) zones and the neighboring oceanic spreading ridges. A Continental Crustal Contamination Trend (CCCT) departing from the basalt compositions of the Mid-Icelandic Belt (MIB) via the Eastern Rift Zone (ERZ) and the Snæfell central volcano at the northern end of the Eastern Flank Zone (EFZ) to Öræfajökull is indicated by yellow shading. Along the well-defined ERZ trend, the distance from the source of individual eruption units to Öræfajökull is generally correlated with the isotope ratios, such that the ERZ samples at the shortest distances are compositionally closest to the EFZ samples. The three guiding lines in the Sr–Pb and Nd–Pb diagrams indicate approximately the inferred progressive melting trends, involving the following basalt series: (*i*) Spitsbergen (Fig. 6*A*) via the western to the eastern Gakkel Ridge in the High Arctic; (*ii*) Snæfellsnes to the Western Rift Zone; (*iii*) Southern Flank Zone via the Reykjanes Peninsula to the Reykjanes Ridge. The isotope ratios of the mantle components EM1 and EM2 are given in each of the diagrams, and the small arrows indicate the approximate directions toward the components. The components are taken as the averages of the most enriched samples with $^{143}Nd/^{144}Nd$ ratios of less than 0.51260 for Pitcairn (EM1) and Samoa (EM2), based on supplementary table 1 in ref. 54. Data sources are as follows: refs. 7, 8, 13–15, and 55–61.

measurements (31). The postulated extension of the JMM—making the total area of the JMM about 100,000 km^2—has wide-reaching implications for the geological evolution of Iceland and adjacent continental margins.

The Iceland Hotspot and Cenozoic Plate Modeling

The Iceland hotspot is widely considered to be sourced by a deep mantle plume from the northern margin of the African large low shear-wave velocity province at the core–mantle boundary (Fig. 6*A*). However, the formation of the North Atlantic Igneous Province has traditionally been attributed to a fixed Iceland plume, with the igneous activity commencing in West Central Greenland in the early Paleocene and relocating to the East Greenland margin at ~40 Ma (Fig. 6*A*) as Greenland moved relative to the Iceland hotspot (32). In our reconstruction, which is based on a global moving hotspot (mantle) reference frame (33), the Iceland plume (Figs. 1 and 6*A*, Table 1, and *Methods*) was beneath East Greenland throughout the early Cenozoic (before 30 Ma). That fits remarkably well with the long-lasting magmatic activity in East Greenland, between 60 and 30 Ma (Fig. 6*B*), in a region that is characterized by thin (<100 km) lithosphere (34). The thinned lithosphere is mostly confined to the Blosseville Kyst (Fig. 6*C*), probably mainly as a result of thermal and mechanical erosion (35) due to the plume head or pulses of magmatic activity in this region between 60 and 35–30 Ma.

Northeast Atlantic seafloor spreading started (chron 24, ~54 Ma) with initial spreading along the Mohn's Ridge, immediately east of the main JMM along the now-extinct Aegir Ridge in the

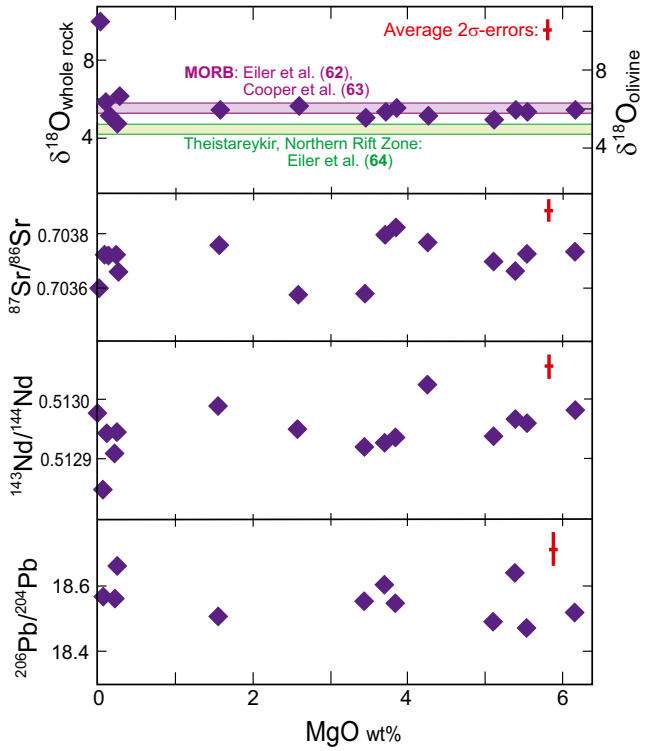

Fig. 4. Isotopic ratios versus MgO concentration for the Öræfajökull compositional range (13) demonstrating the lack of systematic trends. Samples from the Öræfajökull volcanic basement up to 12 My, formed in the older rift zones further west, are not included. The δ^{18}O-range for the Öræfajökull rock suite is generally between or in the ranges for midocean ridge basalts (62, 63) and the most primitive olivine tholeiites and picrites of the Theistareykir volcanic system in the northernmost part of the Northern Rift Zone in Iceland (64). The high δ^{18}O-range for the intermediate and silicic part of the Öræfajökull suite is in strong contrast to the low δ^{18}O of evolved basalts and rhyolites affected by contamination by anatectic melts in the subsiding hydrated basement in the volcanic rift zone systems (19, 65).

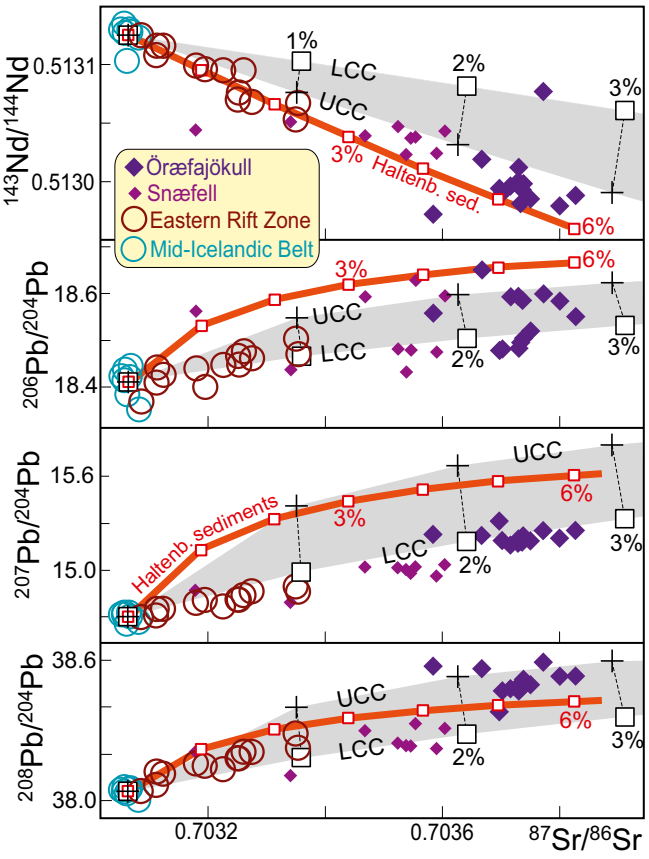

Fig. 5. Mixing models for the Continental Crust Contamination Trend (CCCT), starting from the average composition of Mid-Icelandic Belt (MIB) basalts (14). Only the seven MIB sample localities that do not overlap with the Western, Eastern, and Northern Rift Zones are used. Their average values for Sr–Nd–Pb concentrations and isotope ratios used in the models are 114.86, 5.4457, and 0.25814 ppm, and 0.703064, 0.513075, 18.41086, and 38.03957, respectively. The basalt data for the Eastern Rift Zone and Eastern Volcanic Flank Zone (the Snæfell and Öræfajökull central volcanoes) are as in Fig. 3. Three different contamination models, labeled UCC (upper continental crust), LCC (lower continental crust), and Haltenbanken sediments, are shown. The UCC and LCC components have identical isotope ratios but different trace element concentrations. The isotope ratios are derived from assimilation trends observed in East Greenland Tertiary basalts from the Hold with Hope area (21). The components are chosen to be consistent with the contamination trends defined by the upper series lavas (tables 1C and 3 in ref. 23). The black crosses and squares represent 1% increments of UCC and LCC components with $^{87}Sr/^{86}Sr$, $^{143}Nd/^{143}Nd$, $^{206}Pb/^{204}Pb$, $^{208}Pb/^{204}Pb$, and $^{208}Pb/^{204}Pb$ ratios of 0.712, 0.5122, 18.7, 15.7, and 38.8, respectively. The trace element concentrations of a partially resorbed charnokitic xenolith are not suitable model concentrations due to extensively modified chemistry (23). Instead, we model two alternative sets of element concentrations based on Zartman and Haines (24): (*i*) UCC (black crosses): Sr, Nd, and Pb concentrations of 378, 32, and 23 ppm, respectively, and (*ii*) LCC (black squares): Sr, Nd, and Pb abundances of 389, 14, and 6 ppm, respectively. Generally, these models illustrate that the Snæfell and Öræfajökull basalts could have been derived from basaltic melts with MIB composition by assimilation of 1–3% continental crust of isotopic composition similar to the northeast Greenland contaminants. The exposed continental crust of the central east Greenland Blosseville Kyst (21, 22) has too unradiogenic Pb-isotope compositions to be responsible for the southeast Iceland CC-contamination trend. The alternative Haltenbanken sediment model is based on an average of 116 sediment samples (Dataset S1) from the mid-Norway continental shelf. The $^{87}Sr/^{86}Sr$, $^{143}Nd/^{143}Nd$, $^{206}Pb/^{204}Pb$, and $^{208}Pb/^{204}Pb$ ratios are 0.72587, 0.51197, 18.74, 15.64, and 38.53, and the Sr, Nd, and Pb concentrations are 62, 15, and 15 ppm, respectively. This clastic sediment model results in a higher CC-fraction of 2–6% to yield the Snæfell and Öræfajökull basalts.

Norway Basin, and the Reykjanes Ridge to the south (Fig. 7 *A* and *B*). The fact that seafloor spreading occurred only 8 My after the North Atlantic Igneous Province began forming, and within areas that had undergone extensive stretching, indicates that Iceland plume material probably flowed to the most thinned rifted lithosphere, and triggered continental breakup by upside-down drainage of the plume head (36). In our new plate model, JMM and JMM-E fringed the East Greenland margin until ~52 Mya (Fig. 7*B* and Tables S1 and S2), when the southern part of the northeast Atlantic midocean ridge (Reykjanes) propagated northward and completely detached JMM-E from Greenland by 47 Ma (Fig. 7*C*). At the same time, extension took place east of JMM-E, as a southern continuation of the Norwegian–Greenland Sea. The resulting crust—most likely of oceanic origin—is now covered by younger lavas (the Iceland-Faroe Ridge), which obscure its original characteristics. Due to the competing mid-ocean ridge propagation from the northeast (the Ægir Ridge) and from the southwest (the Reykjanes Ridge) between 50 and 42 Ma, JMM-E experienced rotation, and its boundaries with surrounding continental and oceanic crust were subjected to transpression and strike–slip motion (Fig. S2). This time interval with deforming plates coincides with plate tectonic reorganizations in the northeast Atlantic as witnessed by changes in seafloor spreading directions and rates (27).

Based on the magnetic (Fig. 8*A* and Fig. S2) and gravity signatures and regional plate tectonic configuration, we have

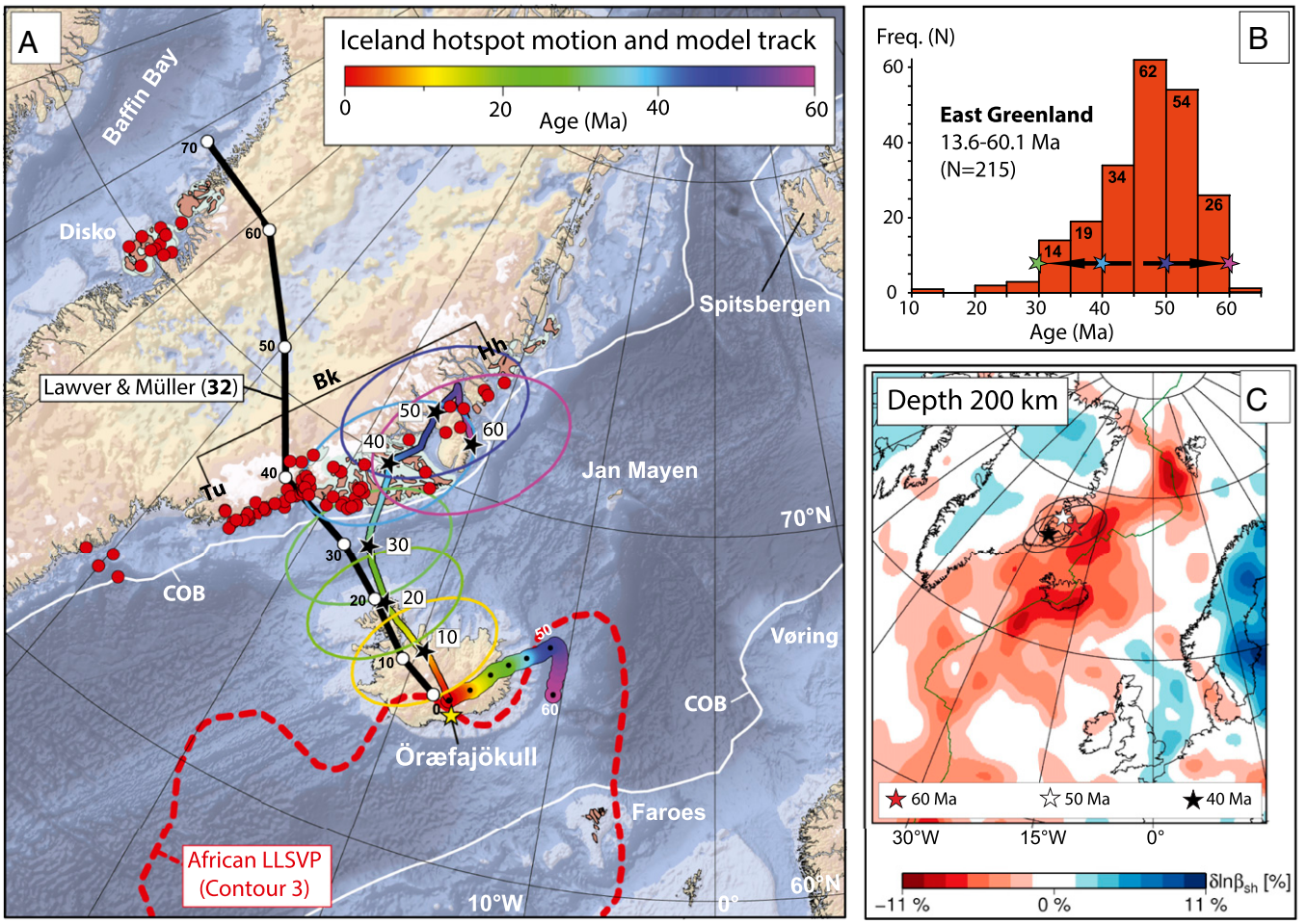

Fig. 6. (*A*) Published onshore and offshore Greenland sample locations (red filled circles) for the North Atlantic Igneous Province isotopic age data (updated from ref. 37), and the predicted location of the Iceland plume relative to the Greenland plate (black star symbols; Table 1) shown at 10-My intervals with 95% confidence ellipses. The surface trace of the Iceland hotspot and the location of the Iceland plume relative to the Greenland plate are both shown as a rainbow-colored swath (color-coded according to age). Our model is compared with the classic fixed-hotspot model of Lawver and Müller (32). Our modeled location for the Iceland plume predicts, within the 95% confidence ellipses, that East Greenland was directly affected by volcanism from about 60 to 30 Ma. For the past 60 My, the Iceland plume (and hotspot motion) when projected vertically downward plots on top of the northern margin of the African Large Low Shear-Wave Velocity Province (LLSVP) near the core–mantle boundary (66, 67), and closest to the seismic voting contour 3 (68). COB (white lines) shows the interpreted transition from continental to oceanic crust. Background bathymetry and subglacial topography map is ETOPO1 (50). Brown areas are above sea level, and blue areas are below sea level. Bk, Blosseville Kyst; Hh, Hold with Hope; Tu, Tugtilik-Sulugssut. (*B*) Histogram showing published isotopic ages from East Greenland (Blosseville Kyst) in 5-My time windows (n = 215 ages). (*C*) The 200-km depth-slice for the horizontally polarized S-wave velocity (β_{sh}) component of the North Atlantic-Instantaneous Phase model of Rickers et al. (34). A low-velocity layer in the offshore regions extends beneath the continental lithosphere of East Greenland, and notably in the area where we predict the location of the Iceland plume between 60 and 40 Ma.

modeled two westward ridge jumps (marked XR52Ma and XR40Ma in Figs. 7 *E* and *F*) and one eastward ridge-jump (XR33Ma in Fig. 7*F*) that are linked to JMM-E. At 40 Ma, the Iceland plume was located beneath Blosseville Kyst (Fig. 1), the only area with substantial volcanism at that time (37). A continuous plate boundary was established west of JMM and JMM-E in the Oligocene (~27 Ma; Fig. 7*F*) by ridge jumps in the direction of the Iceland plume, when the plume impinged the offshore Greenland margin for the first time. The Aegir Ridge became extinct from the south (XR29Ma in Fig. 7*F*) to the northern part of the Norwegian Sea (at 27 Ma), and both JMM and JMM-E became part of the Eurasian plate, where they have resided ever since. The plate boundary was relocated several times (15 and 7 Ma shown in Fig. 8*B*) before establishing its present-day complex configuration within Iceland.

In our model, JMM-E is currently buried under the extensive magmatic infrastructure of Tertiary-to-recent age in southeast Iceland (Fig. 9). Deep burial of crustal material located at the southeast margin of the rift zones might be readily explained by the observations from eastern and western Iceland that older lava piles continuously subside in response to the extensive volcanic loading of the active volcanic zones and their immediate surroundings (38). Despite the continuous plate spreading, the frequent eastward relocations of the Icelandic rift zones at ~24, 15, 7, and 2 Ma (39) enabled slivers of the JMM to remain near the eastern margin of the active rift zone. In a schematic fashion, the right-hand (eastern) part of the lower panel in Fig. 9 can be considered as a section across the currently active Eastern Rift Zone and present plume axis, 33 km west of the Öræfajökull summit (25). The hot plume material will move preferentially toward north and northwest and the magmatically very active Eastern Rift Zone. This is consistent with the continental crustal contamination trend, which is clearly defined by the Eastern Rift Zone basalts.

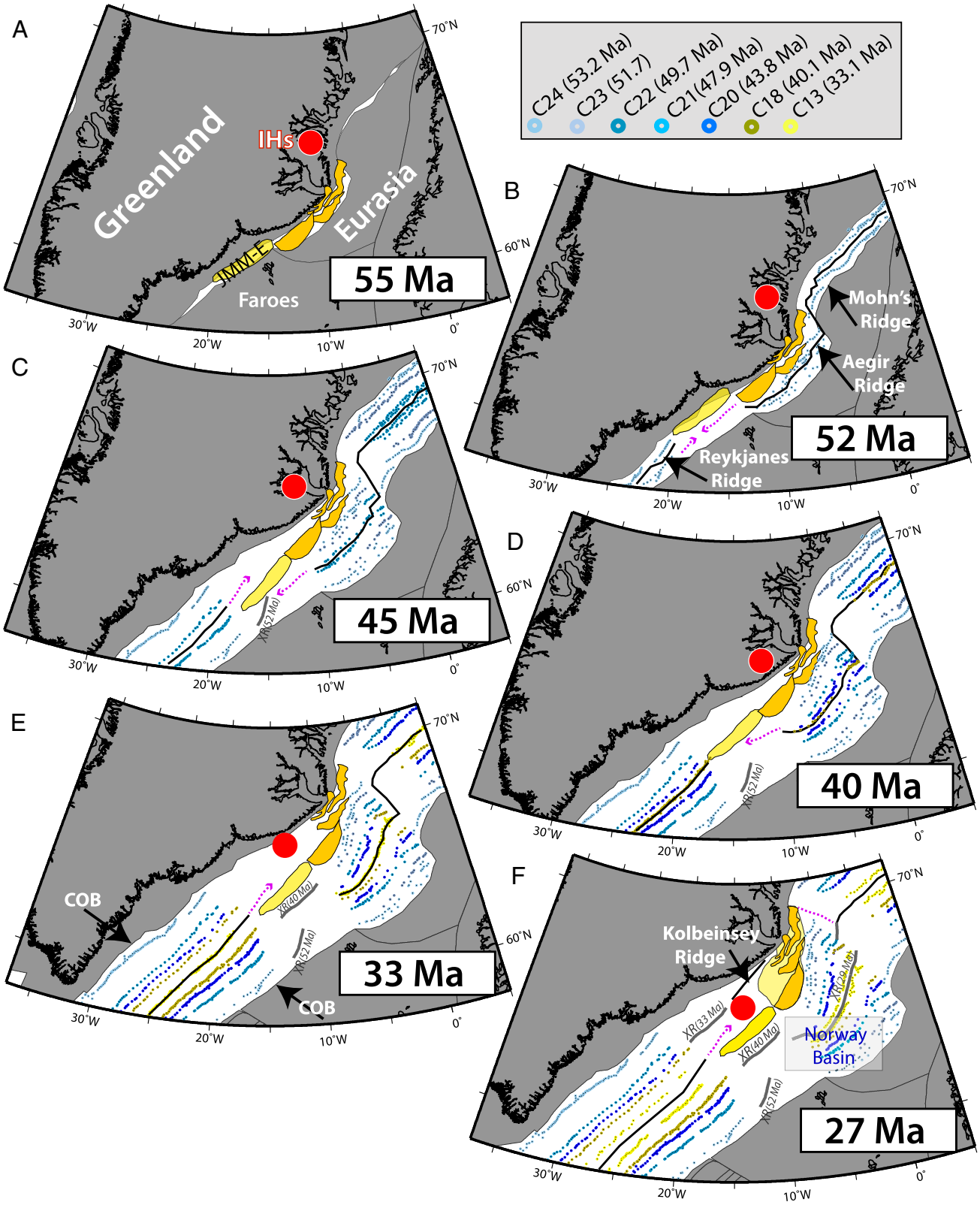

Fig. 7. Series of plate reconstructions (*A–F*) from prebreakup (55 Ma) to 27 Ma. Reconstructed magnetic anomaly picks (C24, C23, C22, C21, C20, C18, and C13) are shown by circles of different colors according to age (69). IHs is the reconstructed position of the Iceland hotspot using an absolute plate model (33). Major continental entities are shown in dark gray, and tectonic boundaries within these regions are indicated as thin gray lines. Main tectonic blocks of JMM are shown in orange, and the estimated southward extension is shown in yellow (JMM-E). Plate boundaries based on magnetic data (Fig. 8*A*) are shown as black lines, and suggested locations of plate boundaries in regions where the magnetic data are ambiguous are shown as dashed magenta lines. Abandoned midocean ridges (XR) are shown as thick gray lines. Light yellow area around the main JMM blocks indicates extended continental crust. COB indicates the transition from continental to oceanic crust.

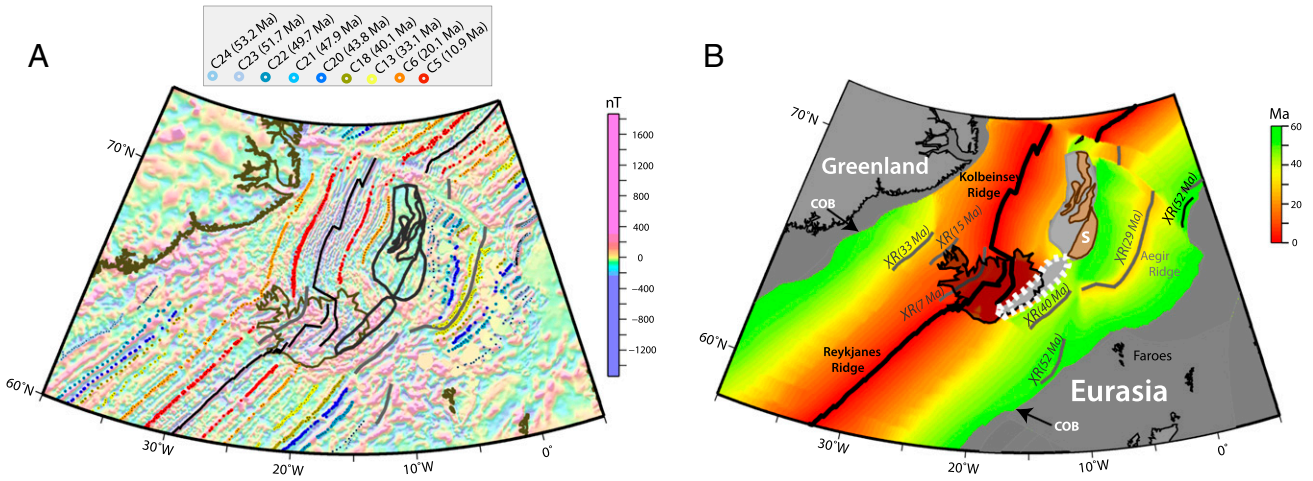

Fig. 8. (*A*) Magnetic anomaly grid of the northeast Atlantic (26) and selected magnetic picks for normal chrons (C24, C23, C22, C21, C20, C18, C13, C6, and C5) according to ref. 69. (*B*) Present-day age of oceanic crust based on dense marine magnetic anomaly interpretation and location of observed and inferred extinct midocean ridges. Interpreted continental blocks of JMM are outlined in brown (reconstruction parameters for block S differ slightly from the other JMM blocks; Tables S1 and S2), and light gray indicates added extended continental crust (including the postulated JMM-E outlined by the dashed white line). The ocean-age isochrons were used to determine the lithosphere thermal gravity anomaly correction in gravity inversion (Figs. 1 and 2*B*, and Figs. S3 and S4). XR, extinct midocean ridges; COB, the suggested limit between continental and oceanic crust.

Ocean Island Basalts, Enriched Geochemical Signatures, and Lost Continents

Recycling of continental material through the deep mantle (40) has been invoked to explain many enriched geochemical signatures of Ocean Island Basalts (OIB), but that explanation is based on the assumption that OIB are underlain largely by oceanic lithosphere. However, there are numerous examples of continental fragments within the oceanic basins. Some can be

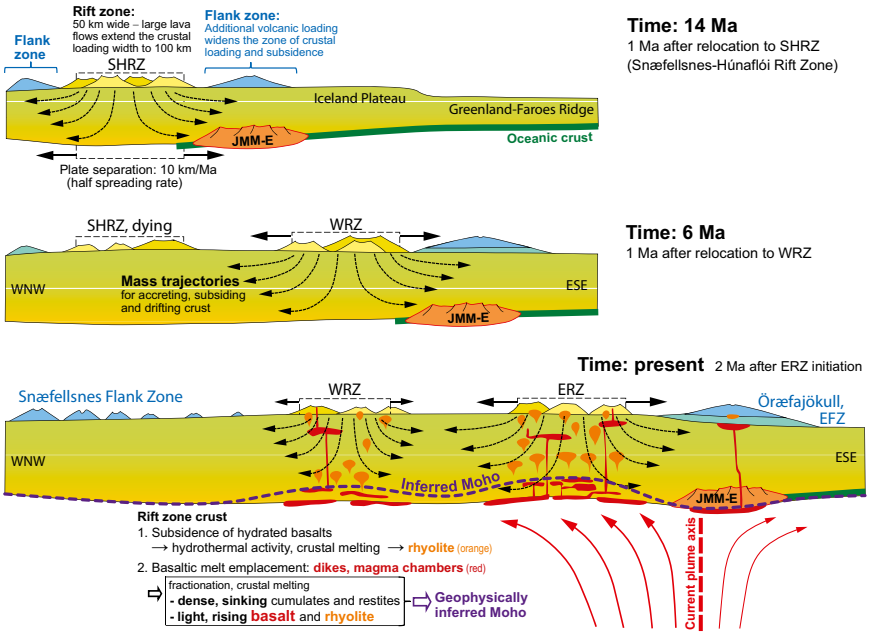

Fig. 9. Simplified and schematic west-northwest–east-southeast–trending cross-sections through the Icelandic crust, demonstrating the mechanism of successive cycles of deep burial of continental slivers of the extended Jan Mayen Microcontinent (JMM-E). The cross-sections are not drawn to exact scale. The location of the lower section through the plume axis is shown in Fig. 2*A*. The observations that older lava piles west and east of the rift zones strike parallel to and dip gently toward the nearest rift zone (38, 70), indicate continuous subsidence resulting from extensive volcanic loading of the rift zone and immediately surrounding crust. The volcanic activity in the flank zones produces additional loading and crustal burial 50–100 km outside the rift zones, which have jumped eastward every 5–9 My, at about 24, 15, 7, and 2 Ma (39), in response to the westward migration of the northeast Atlantic plate boundary relative to the plume axis. The JMM-E, positioned east of the plume at 27 Ma (Fig. 7*F*), could therefore remain within about 70 km of the nearest rift zone margin until today. The three sections depict the rift zone configurations and state of the JMM-E burial at 14, 6, and 0 Ma. The rate of burial is highest when the JMM-E is close to the rift zone margins, within the first 2–3 My of rift zone relocation. The current plume axis (25), plume flow pattern, and inferred Moho (Fig. 2*B* and ref. 46) are shown in the lower panel (present), which also indicates how the magmatic processes under the rift zones produce intracrustal segregation of light, rising melts from dense, sinking cumulates and restites. This may cause the observed shallowing of the Moho under the rift zones (46). EFZ, Eastern Flank Zone; WRZ, ERZ, and SHRZ: Western, Eastern, and Snæfellsnes-Húnaflói Rift Zone.

readily detected by examining outcrops (e.g., Seychelles) or from geophysical data, e.g., JMM (26–29, 31) and the Laxmi Ridge (41) in the northeast Indian Ocean, or from analyses of mantle xenoliths (42). Others, such as the postulated Mauritia Microcontinent (43), may be obscured by thick successions of younger volcanic material. Samples of old continental crust dredged or drilled from some locations thought to be exclusively represented by OIB, e.g., Kerguelen (44), suggest the occurrence of continental fragments, and that many OIBs assimilated some continental material during the passage of melts through the lithosphere. The geochemical signatures of the Öræfajökull lavas bear witness to this, and an extension of the JMM beneath Öræfajökull also explains the surprisingly thick crust in southeast Iceland. We calculate a maximum crustal thickness of around 32 km, which fits well with seismic refraction results and receiver function analysis (10, 45, 46) (Fig. S4). The thick crust is predicted to extend offshore in a northeast direction (Figs. 1 and 2*B*), forming a region of anomalously thick crust protruding into the oceanic crust of the Norwegian Sea, which is to the north of (but distinct from) the Iceland-Faroe Ridge. The postulated extension of the JMM beneath Iceland points out that intraoceanic continental fragments are more abundant than previously thought, and caution is therefore recommended in relating enriched geochemical signatures in OIBs to recycled material in mantle plumes.

Methods

Haltenbanken Isotope Analysis. Sr, Nd, and Pb isotope analyses of 116 sediment whole-rock samples from Haltenbanken, Mid-Norwegian shelf (Dataset S1), were carried out by Isotopic Analytical Services, Ltd., in Aberdeen, Scotland. Sediment samples were crushed and ground to fine powder and dissolved in HF. Rb, Sr, Sm, Nd, and Pb were separated using ion-exchange chromatography, and isotope ratios were measured by thermal ionization mass spectrometry using two VG Sector 54 fully automated thermal ionization mass spectrometers. Rb, Sr, Sm, and Nd concentrations were determined by isotope dilution, and Pb, Th, and U concentrations were determined by inductively coupled plasma mass spectrometry.

Location of the Iceland Hotspot. The fixed-hotspot and moving-hotspot tracks (Figs. 1 and 6*A*, and Table 1) presented here are different for several reasons: one is the motion of the Iceland hotspot itself (Fig. 6*A*); another is the difference in the reference frame, which is due to the motion of those hotspots (other than Iceland) on which the reference frames are based. The fixed-hotspot frame (32) was only based on Indo-Atlantic hotspots (47), whereas the moving-hotspot reference frame (33) is global and based on Indo-Atlantic (Tristan, Reunion, New England) and Pacific (Hawaii and Louisville) hotspots. Relative plate circuits also differ between the two models and relative plate kinematics within the North Atlantic are based on marine magnetic anomalies (Fig. 8*A* and Fig. S2), fracture zones, and estimates of prebreakup extension (27, 48). For the past 30 My, the two models agree within error (Fig. 6*A*). The uncertainty ellipses correspond to 95% uncertainties for the finite rotations describing the motion of Greenland in the global moving-hotspot reference frame. These uncertainties were not combined with the uncertainties of the Greenland–North America–Africa relative motion because uncertainties in the plate circuits are negligible compared with the large uncertainties of the hotspot reference frame itself (Africa relative to hotspots), and uncertainties in motion of the Iceland hotspot itself were not considered either. We do not assume any specific present-day uncertainty of the Iceland hotspot, but for the five hotspots on which we base the hotspot reference frame, these are 150–200 km (and increasing in the past), and they percolate into the uncertainties of hotspot reference frame rotations.

A present-day plume location of 64.4°N and 17°W (Figs. 1 and 6*A*) was used for plume modeling by Doubrovine et al. (33). The plume position of Shorttle et al. (25) at 63.95°N, 17.4°W (Fig. 2*A*), is located 54 km SSW from the original modeling location but makes it easier to explain the continental crustal contamination trend caused by the JMM-E.

Crustal Thickness. Gravity anomaly inversion to determine Moho depth, crustal basement thickness (Figs. 1 and 2*B*, and Figs. S3 and S4), and continental lithosphere thinning for the northeast Atlantic adjacent to Iceland incorporate a lithosphere thermal gravity anomaly correction for both oceanic and continental lithosphere. The calculation of the continental lithosphere thinning using gravity correction incorporates an adjustment for magmatic addition due to decompression melting during breakup and seafloor spreading. Data used in the gravity inversion are public domain free-air gravity data (49), bathymetry (50), sediment thickness (51, 52), and revised ocean isochrons (Fig. 8*B*). The gravity inversion for Moho depth and hence crustal basement thickness requires a constant density contrast between crustal basement and mantle. For the mantle and crust, we use a density of 3,300 and 2,850 $kg{\cdot}m^{-3}$, respectively. The long wavelength components of the Earth's gravity anomaly field are controlled by mantle dynamic processes, and as a consequence, the reference Moho depth used in the gravity inversion must be calibrated against independent seismic refraction Moho depths. A reference Moho depth of 35 km has been used in this study. The gravity inversion methodology is described in detail in refs. 29, 30, 43, and 53.

ACKNOWLEDGMENTS. We thank Statoil for releasing the Haltenbanken Sr–Nd–Pb data (Dataset S1), and A. W. Hofmann, the handling editor, and an anonymous reviewer for constructive and helpful reviews. The European Research Council under the European Union's Seventh Framework Programme (FP7/2007-2013)/European Research Council Advanced Grant Agreement 267631 (Beyond Plate Tectonics) and the Research Council of Norway through its Centres of Excellence funding scheme (Centre for Earth Evolution and Dynamics, 223272) are acknowledged for financial support.

1. Ganerød M, et al. (2010) The North Atlantic Igneous Province reconstructed and its relation to the Plume Generation Zone: The Antrim Lava Group revisited. *Geophys J Int* 182:183–202.
2. White RS, McKenzie DP (1995) Mantle plumes and flood basalts. *J Geophys Res* 100(B9):17543–17585.
3. Starkey NA, et al. (2009) Helium isotopes in early Iceland plume picrites: Constraints on the composition of high $^3He/^4He$ mantle. *Earth Planet Sci Lett* 277:91–100.
4. Jackson MG, et al. (2010) Evidence for the survival of the oldest terrestrial mantle reservoir. *Nature* 466(7308):853–856.
5. Debaille V, et al. (2009) Primitive off-rift basalts from Iceland and Jan Mayen: Os-isotopic evidence for a mantle source containing enriched subcontinental lithosphere. *Geochim Cosmochim Acta* 73(11):3423–3449.
6. Hanan BB, Blichert-Toft J, Kingsley R, Schilling J-G (1999) Depleted Iceland mantle plume geochemical signature: Artefact of multicomponent mixing? *Geochem Geophys Geosyst* 1(4):GC000009.
7. Thirlwall MF, Gee MAM, Taylor RN, Murton BJ (2004) Mantle components in Iceland and adjacent ridges investigated using double-spike Pb isotope ratios? *Geochim Cosmochim Acta* 68(2):361–386.
8. Peate DW, et al. (2010) Compositional characteristics and spatial distribution of enriched Icelandic mantle components. *J Petrol* 51(7):1447–1475.
9. Schaltegger U, et al. (2002) Contamination of OIB by underlying ancient continental lithosphere: U-Pb and Hf isotopes in zircons question EM1 and EM2 mantle components. *Geochimica et Cosmochimica Acta*: Volume 66, Supplement 1, A673.
10. Foulger GR (2006) Older crust underlies Iceland. *Geophys J Int* 165:672–676.
11. Paquette J, Sigmarsson O, Tiepolo M (2006) Continental basement under Iceland revealed by old zircons. *Eos Trans AGU*, 2006AGUFM.V33A0642P.
12. Hart SR (1984) A large-scale isotope anomaly in the Southern Hemisphere mantle. *Nature* 309:753–757.
13. Prestvik T, Goldberg S, Karlsson H, Grönvold K (2001) Anomalous strontium and lead isotope signatures in the off-rift Oraefajokull central volcano in south-east Iceland. Evidence for enriched endmember(s) of the Iceland mantle plume? *Earth Planet Sci Lett* 190:211–220.
14. Kokfelt TF, et al. (2006) Combined trace element and Pb-Nd-Sr-O isotope evidence for recycled oceanic crust (upper and lower) in the Iceland mantle plume. *J Petrol* 47(9): 1705–1749.
15. Manning CJ, Thirlwall MF (2014) Isotopic evidence for interaction between Öræfajökull mantle and the Eastern Rift Zone, Iceland. *Contrib Mineral Petrol,* 167(1), 10.1007/s00410-013-0959-1–22.
16. Jackson MG, et al. (2007) The return of subducted continental crust in Samoan lavas. *Nature* 448(7154):684–687.
17. Selbekk RS, Trønnes RG (2007) The 1362 AD plinian Öræfajökull eruption, Iceland: Petrology and geochemistry of large-volume homogeneous rhyolitic. *J Volcanol Geotherm Res* 160:45–57.
18. Martin E, Sigmarsson O (2010) Thirteen million years of silicic magma production in Iceland: Links between petrogenesis and tectonic settings. *Lithos* 116:129–144.
19. Bindeman I, et al. (2012) Silicic magma petrogenesis in Iceland by remelting of hydrothermally altered crust based on oxygen isotope diversity and disequilibria between zircon and magma with implications for MORB. *Terra Nova* 24(3):227–232.
20. Trønnes RG, Debaille V, Erambert M, Stuart FM, Waight T (2013) Mixing and progressive melting of deep and shallow mantle sources in the NE Atlantic and Arctic (abstract, Goldschmidt Conf.). *Mineral Mag* 77:2357.

21. Peate DW, Barker AK, Riishuus MS, Andreasen R (2008) Temporal variations in crustal assimilation of magma suites in the East Greenland flood basalt province: Tracking the evolution of magmatic plumbing systems. *Lithos* 102:179–197.
22. Hansen H, Nielsen TFD (1999) Crustal contamination in Palaeogene East Greenland flood basalts: Plumbing system evolution during continental rifting. *Chem Geol* 157: 89–118.
23. Thirlwall M, Upton BGJ, Jenkins C (1994) Interaction between continental lithosphere and the Iceland plume—Sr–Nd–Pb isotope geochemistry of Tertiary basalts, NE Greenland. *J Petrol* 35(3):839–879.
24. Zartman RE, Haines SM (1988) The plumbotectonic model for Pb isotopic systematics among major terrestrial reservoirs—a case for bi-directional transport. *Geochim Cosmochim Acta* 52(6):1327–1339.
25. Shorttle O, Maclennan J, Jones SM (2010) Control of the symmetry of plume-ridge interaction by spreading ridge geometry. *Geochem Geophys Geosyst* 11(7):Q0AC05.
26. Gaina C, Werner SC, Saltus R, Maus S, CAMP-GM Group (2011) Circum-Arctic Mapping Project: New magnetic and gravity anomaly maps of the Arctic. *Arctic Petroleum Geology*, eds Spencer AM, Embry AF, Gautier DL, Stoupakova AV, Sørensen K, Geological Society London, Memoirs (Geological Society, London), Vol 35, pp 39–48.
27. Gaina C, Gernigon L, Ball P (2009) Palaeocene: Recent plate boundaries in the NE Atlantic and the formation of the Jan Mayen microcontinent. *J Geol Soc Lond* 166: 601–616.
28. Peron-Pinvidic G, Gernigon L, Gaina C, Ball P (2012) Insights from the Jan Mayen system in the Norwegian–Greenland Sea—II. Architecture of a microcontinent. *Geophys J Int* 191:413–435.
29. Greenhalgh EE, Kusznir NJ (2007) Evidence for thin oceanic crust on the extinct Aegir Ridge, Norwegian Basin, NE Atlantic derived from satellite gravity inversion. *Geophys Res Lett* 34(6):L06305.
30. Chappell AR, Kusznir NJ (2008) Three-dimensional gravity inversion for Moho depth at rifted continental margins incorporating a lithosphere thermal gravity anomaly correction. *Geophys J Int* 174:1–13.
31. Breivik AJ, Mjelde R, Faleide JI, Muro Y (2012) The eastern Jan Mayen microcontinent volcanic margin. *Geophys J Int* 188:798–818.
32. Lawver LA, Müller RD (1994) Iceland hotspot track. *Geology* 22(4):311–314.
33. Doubrovine PV, Steinberger B, Torsvik TH (2012) Absolute plate motions in a reference frame defined by moving hot spots in the Pacific, Atlantic, and Indian oceans. *J Geophys Res* 117(B9):B09101.
34. Rickers F, Fichtner A, Trampert J (2013) The Iceland-Jan Mayen plume system and its impact on mantle dynamics in the North Atlantic region: Evidence from full-waveform inversion. *Earth Planet Sci Lett* 367:39–51.
35. Steinberger B, Spakman W, Japsen P, Torsvik TH (2014) The key role of global solid-Earth processes in preconditioning Greenland's glaciation since the Pliocene. *Terra Nova* 27(1):1–8.
36. Sleep NH (1997) Lateral flow and ponding of starting plume material. *J Geophys Res* 102(B5):10001–10012.
37. Torsvik TH, Mosar J, Eide EA (2001) Cretaceous–Tertiary geodynamics: A North Atlantic exercise. *Geophys J Int* 146:850–866.
38. Bodvarsson G, Walker GPL (1964) Crustal drift in Iceland. *Geophys J R Astron Soc* 8: 285–300.
39. Harðarson BS, Fitton JG, Hjartarson Á (2008) Tertiary volcanism in Iceland. *Jökull* 58: 161–178.
40. Hofmann AW (1997) Mantle geochemistry: The message from oceanic volcanism. *Nature* 385(6612):219–229.
41. Collier JS, et al. (2009) Factors influencing magmatism during continental breakup: New insights from a wide-angle seismic experiment across the conjugate Seychelles-Indian margins. *J Geophys Res* 114(B3):(B03101)1–25.
42. Coltorti M, Bonadiman C, O'Reilly SY, Griffin WL, Pearson NJ (2010) Buoyant ancient continental mantle embedded in oceanic lithosphere (Sal Island, Cape Verde Archipelago). *Lithos* 120:223–233.
43. Torsvik TH, et al. (2013) A Precambrian microcontinent in the Indian Ocean. *Nat Geosci* 6:223–227.
44. Frey FA, Weis D, Borisova AY (2002) Involvement of continental crust in the formation of the Cretaceous Kerguelen Plateau: New perspectives from ODP Leg 120 sites. *J Petrol* 43(7):1207–1239.
45. Darbyshire FA, White RS, Priestley KF (2000) Structure of the crust and uppermost mantle of Iceland from a combined seismic and gravity study. *Earth Planet Sci Lett* 181:409–428.
46. Kumar P, Kind R, Priestley K, Dahl-Jensen T (2007) Crustal structure of Iceland and Greenland from receiver function studies. *J Geophys Res* 112(B3):(B03301)1–19.
47. Müller RD, Royer J-Y, Lawver LA (1993) Revised plate motions relative to the hotspots from combined Atlantic and Indian Ocean hotspot tracks. *Geology* 21(3):275–278.
48. Torsvik TH, Müller RD, Van der Voo R, Steinberger B, Gaina C (2008) Global plate motion frames: Toward a unified model. *Rev Geophys* 46(3):RG3004.
49. Sandwell DT, Smith WHF (2009) Global marine gravity from retracked Geosat and ERS-1 altimetry: Ridge segmentation versus spreading rate. *J Geophys Res* 114: B01411.
50. Amante C, Eakins BW (2009) ETOPO1, 1 Arc-Minute Global Relief Model: Procedures, data sources and analysis. NOAA Technical Memorandum NESDIS NGDC-24 (National Oceanic and Atmospheric Administration, Washington, DC).
51. Divins DL (2008) Total sediment thickness of the World's oceans and marginal seas. NGDC. Available at https://www.ngdc.noaa.gov/mgg/sedthick/sedthick.html. Accessed May 21, 2014.
52. Laske G, Masters G (1997) A global digital map of sediment thickness. *Eos Trans AGU* 78:F483.
53. Alvey A, Gaina C, Kusznir NJ, Torsvik TH (2008) Integrated crustal thickness mapping and plate reconstructions for the High Arctic. *Earth Planet Sci Lett* 274:310–321.
54. Stracke A (2012) Earth's heterogeneous mantle: A product of convection-driven interaction between crust and mantle. *Chem Geol* 330-331:274–299.
55. Peate DW, et al. (2009) Historic magmatism on the Reykjanes Peninsula, Iceland: A snap-shot of melt generation at a ridge segment. *Contrib Mineral Petrol* 157:359–382.
56. Goldstein SL, et al. (2008) Origin of a "Southern Hemisphere" geochemical signature in the Arctic upper mantle. *Nature* 453(7191):89–93.
57. Schilling J-G, Kingsley R, Fontignie D, Poreda R, Xue S (1999) Dispersion of the Jan Mayen and Iceland mantle plumes in the Arctic: A He-Pb-Nd-Sr isotope tracer study of basalts from the Kolbeinsey, Mohns, and Knipovich Ridges. *J Geophys Res* 104(B5): 10543–10569.
58. Stracke A, et al. (2003) Theistareykir revisited. *Geochem Geophys Geosyst* 4(2): 2001GC000201.
59. Blichert-Toft J, et al. (2005) Geochemical segmentation of the mid-Atlantic ridge north of Iceland and ridge-hot spot interaction in the north Atlantic. *Geochem Geophys Geosyst* 6(1):Q01E19.
60. Shorttle O, Maclennan J, Piotrowski AM (2013) Geochemical provincialism in the Iceland plume. *Geochim Cosmochim Acta* 122:363–397.
61. Ionov DA, Mukasa SB, Bodinier L-J (2002) Sr-Nd-Pb isotopic compositions of peridotite xenoliths from Spitsbergen: Numerical modelling indicates Sr-Nd decoupling in the mantle by melt percolation metasomatism. *J Petrol* 43(12):2261–2278.
62. Eiler JM, Schiano P, Kitchen N, Stolper EM (2000) Oxygen-isotope evidence for recycled crust in the sources of mid-ocean-ridge basalts. *Nature* 403(6769):530–534.
63. Cooper KM, Eiler JM, Asimow PD, Langmuir CH (2004) Oxygen isotope evidence for the origin of enriched mantle beneath the mid-Atlantic ridge. *Earth Planet Sci Lett* 220:279–316.
64. Eiler JM, Grönvold K, Kitchen N (2000) Oxygen isotope evidence for the origin of chemical variations in lavas from Theistareykir volcano in Iceland's northern volcanic zone. *Earth Planet Sci Lett* 184:269–286.
65. Nicholson H, et al. (1991) Geochemical and Isotopic evidence for crustal assimilation beneath Krafla, Iceland. *J Petrol* 32(5):1005–1020.
66. Torsvik TH, Burke K, Steinberger B, Webb SJ, Ashwal LD (2010) Diamonds sampled by plumes from the core-mantle boundary. *Nature* 466(7304):352–355.
67. Torsvik TH, et al. (2014) Deep mantle structure as a reference frame for movements in and on the Earth. *Proc Natl Acad Sci USA* 111(24):8735–8740.
68. Lekic V, Cottar S, Dziewonski A, Romanowicz B (2012) Cluster analysis of global lower mantle tomography: A new class of structure and implications for chemical heterogeneity. *Earth Planet Sci Lett* 357:68–77.
69. Cande SC, Kent DV (1995) Revised calibration of the geomagnetic polarity timescale for the Late Cretaceous and Cenozoic. *J Geophys Res* 100(B4):6093–6095, 10.1029/94JB03098.
70. Pálmason G (1973) Kinematics and heat flow in a volcanic rift zone, with application to Iceland. *Geophys J R Astron Soc* 33:451–481.

Supporting Information

Torsvik et al. 10.1073/pnas.1423099112

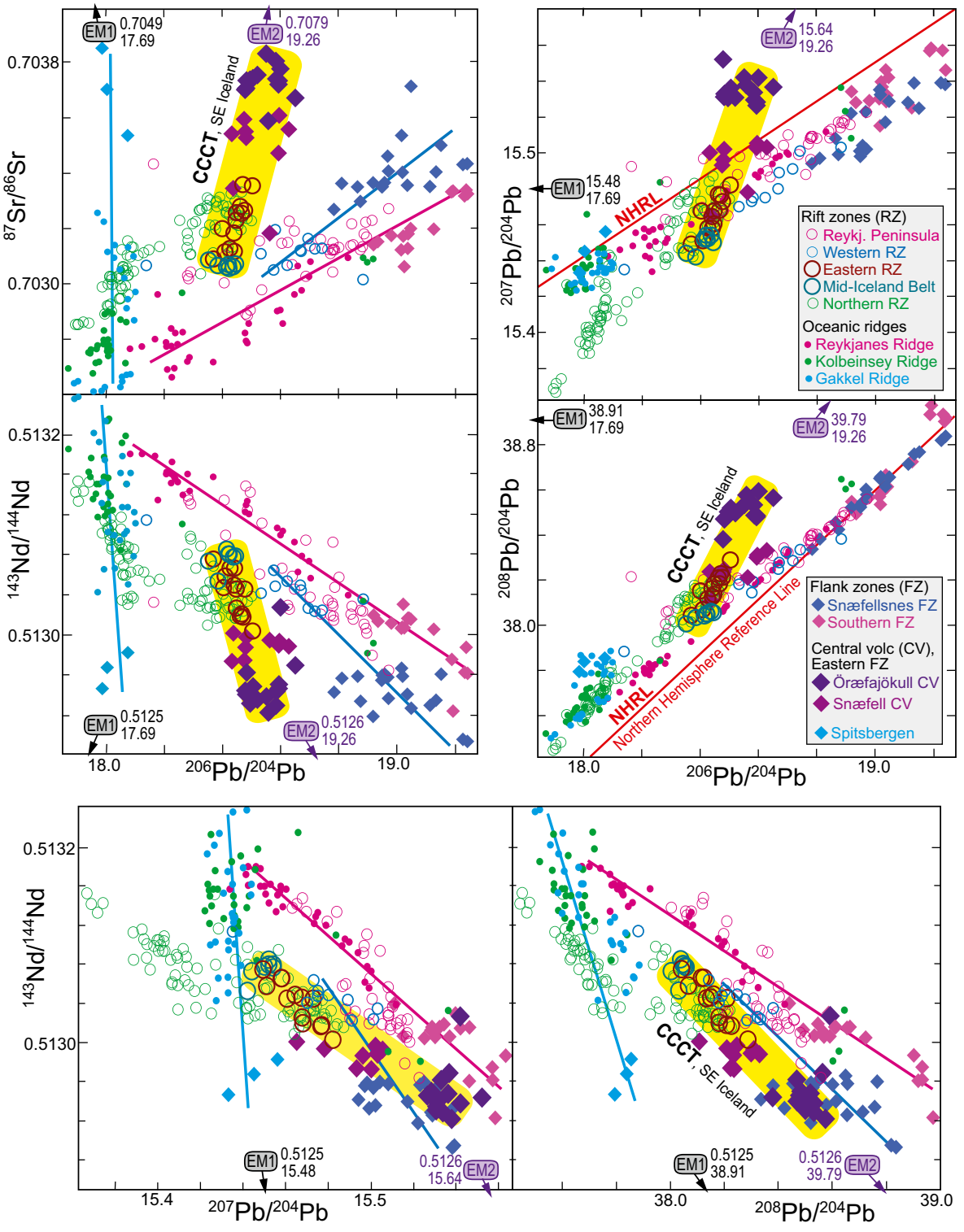

Fig. S1. (Expanded version of Fig. 3.) The Sr–Nd–Pb isotopic composition of basalts from the Icelandic rift and off-rift (flank) zones and the neighboring oceanic spreading ridges. A Continental Crustal Contamination Trend (CCCT) departing from the basalt compositions of the Mid-Icelandic Belt (MIB) via the

Legend continued on following page

Eastern Rift Zone (ERZ) and the Snæfell central volcano at the northern end of the Eastern Flank Zone (EFZ) to Öræfajökull is indicated by yellow shading. Along the well-defined ERZ trend, the distance from the source of individual eruption units to Öræfajökull is generally correlated with the isotope ratios, such that the ERZ samples at the shortest distances are compositionally closest to the EFZ samples. The three guiding lines in the Sr–Pb and Nd–Pb diagrams indicate approximately (not strictly linear regression) the inferred progressive melting trends, involving the following basalt series: (*i*) Spitsbergen via the western to the eastern Gakkel Ridge in the High Arctic; (*ii*) Snæfellsnes to the Western Rift Zone; (*iii*) Southern Flank Zone via the Reykjanes Peninsula to the Reykjanes Ridge. The isotope ratios of the mantle components EM1 and EM2 are given in the each of the diagrams, and the small arrows indicate the approximate directions toward the components. The components are taken as the averages of the most enriched samples with $^{143}Nd/^{144}Nd$ ratios of less than 0.51260 for Pitcairn (EM1) and Samoa (EM2) based on the supplementary table 1 in ref. 1. Data sources are refs. 2–13. Apart from the CCCT from MIB toward the Öræfajökull basalts, the compositional range of basalts from Iceland and the northeast Atlantic and Arctic Oceans can be modeled by mixing and progressive melting of mantle sources, including the Iceland plume with 10% recycled oceanic crust (ROC) and 90% of a diverse lower mantle (containing both melt-depleted and fertile components) and local asthenosphere, contaminated by subcontinental lithospheric mantle (SCLM) (14, 15). The proportion of SCLM increases north of Iceland (the Kolbeinsey, Mohns, and Knipovich Ridges and the Jan Mayen area) and predominates in the Pleistocene to Holocene basalts from Spitsbergen and along the Gakkel Ridge (13–15). The Sr–Pb and Nd–Pb isotope diagrams illustrate various progressive melting trends from fertile to depleted basalts, characterized by variable ROC/SCLM ratios. The highest ROC/SCLM ratio is found in the Southern Flank Zone (SFZ) and the Snæfellsnes Flank Zone, melting to form more depleted basalts of the Reykjanes Peninsula and Ridge and the Western Rift Zone, respectively. The melting trends displayed by basalts from Jan Mayen Island and Jan Mayen Plateau toward the Mohns and Knipovich Ridges (ref. 14; not shown here) represent intermediate ROC/SCLM ratios, whereas the trend from Spitsbergen via the western to the eastern parts of the Gakkel Ridge (High Arctic) have the lowest ROC/SCLM ratios, approaching zero. The Spitsbergen to Gakkel and Southern FZ to Reykjanes melting trends merge at the depleted end of the mid-ocean ridge basalt compositional spectrum, characterized by high Nd- and low Sr- and Pb-isotope ratios. A series of subparallel trends, i.e., from Snæfellsnes FZ via the Western RZ, Northern RZ, and Kolbeinsey Ridge and from Jan Mayen to the Mohns and Knipovich Ridges (not shown), are located between the two extreme Gakkel and Reykjanes melting trends in the various Sr–Pb and Nd–Pb isotope diagrams. The uniqueness of the CCCT is indicated by the fact that it variably intersects the other trends in Sr–Pb and Nd–Pb isotope space. The most prominent feature of the three Nd–Pb diagrams is that the Öræfajökull end of the CCCT points toward low $^{206}Pb/^{204}Pb$, high $^{207}Pb/^{204}Pb$, and intermediate $^{208}Pb/^{204}Pb$ with decreasing $^{143}Nd/^{144}Nd$, e.g., relative to the trend from the Snæfellsnes FZ to the Western RZ. The very low $^{207}Pb/^{204}Pb$ ratios of the picritic lavas from the northern part of the Northern Rift Zone (6) indicate extensive melting of a plume-supplied lower mantle source that was subjected to strong melt depletion early in Earth's history.

1. Stracke A (2012) Earth's heterogeneous mantle: A product of convection-driven interaction between crust and mantle. *Chem Geol* 330-331:274–299.
2. Prestvik T, Goldberg S, Karlsson H, Grönvold K (2001) Anomalous strontium and lead isotope signatures in the off-rift Öræfajökull central volcano in south-east Iceland. Evidence for enriched endmember(s) of the Iceland mantle plume? *Earth Planet Sci Lett* 190:211–220.
3. Kokfelt TF, et al. (2006) Combined trace element and Pb-Nd-Sr-O isotope evidence for recycled oceanic crust (upper and lower) in the Iceland mantle plume. *J Petrol* 47(9):1705.
4. Peate DW, et al. (2010) Compositional characteristics and spatial distribution of enriched Icelandic mantle components. *J Petrol* 51(7):1447–1475.
5. Schilling J-G, Kingsley R, Fontignie D, Poreda R, Xue S (1999) Dispersion of the Jan Mayen and Iceland mantle plumes in the Arctic: A He-Pb-Nd-Sr isotope tracer study of basalts from the Kolbeinsey, Mohns, and Knipovich Ridges. *J Geophys Res* 104:10543–10569.
6. Stracke A, et al. (2003) Theistareykir revisited. *Geochem Geophys Geosyst* 4:2001GC000201.
7. Thirlwall MF, Gee MAM, Taylor RN, Murton BJ (2004) Mantle components in Iceland and adjacent ridges investigated using double-spike Pb isotope ratios. *Geochim Cosmochim Acta* 68(2):361–386.
8. Manning CJ, Thirlwall MF (2014) Isotopic evidence for interaction between Öræfajökull mantle and the Eastern Rift Zone, Iceland. *Contrib Mineral Petrol* 167(1):10.1007/s00410-013-0959-1–22.
9. Blichert-Toft J, et al. (2005) Geochemical segmentation of the mid-Atlantic ridge north of Iceland and ridge-hot spot interaction in the north Atlantic. *Geochem Geophys Geosyst* 6(1): Q01E19.
10. Peate DW, et al. (2009) Historic magmatism on the Reykjanes Peninsula, Iceland: A snap-shot of melt generation at a ridge segment. *Contrib Mineral Petrol* 157:359–382.
11. Shorttle O, Maclennan J, Piotrowski AM (2013) Geochemical provincialism in the Iceland plume. *Geochim Cosmochim Acta* 122:363–397.
12. Ionov DA, Mukasa SB, Bodinier J-L (2002) Sr-Nd-Pb isotopic compositions of peridotite xenoliths from Spitsbergen: Numerical modelling indicates Sr-Nd decoupling in the mantle by melt percolation metasomatism. *J Petrol* 43(12):2261–2278.
13. Goldstein SL, et al. (2008) Origin of a "Southern Hemisphere" geochemical signature in the Arctic upper mantle. *Nature* 453(7191):89–93.
14. Trønnes RG, Debaille V, Erambert M, Stuart FM, Waight T (2013) Mixing and progressive melting of deep and shallow mantle sources in the NE Atlantic and Arctic (abstract, Goldschmidt Conf.). *Mineral Mag* 77:2357.
15. Debaille V, et al. (2009) Primitive off-rift basalts from Iceland and Jan Mayen: Os-isotopic evidence for a mantle source containing enriched subcontinental lithosphere. *Geochim Cosmochim Acta* 73(11):3423–3449.

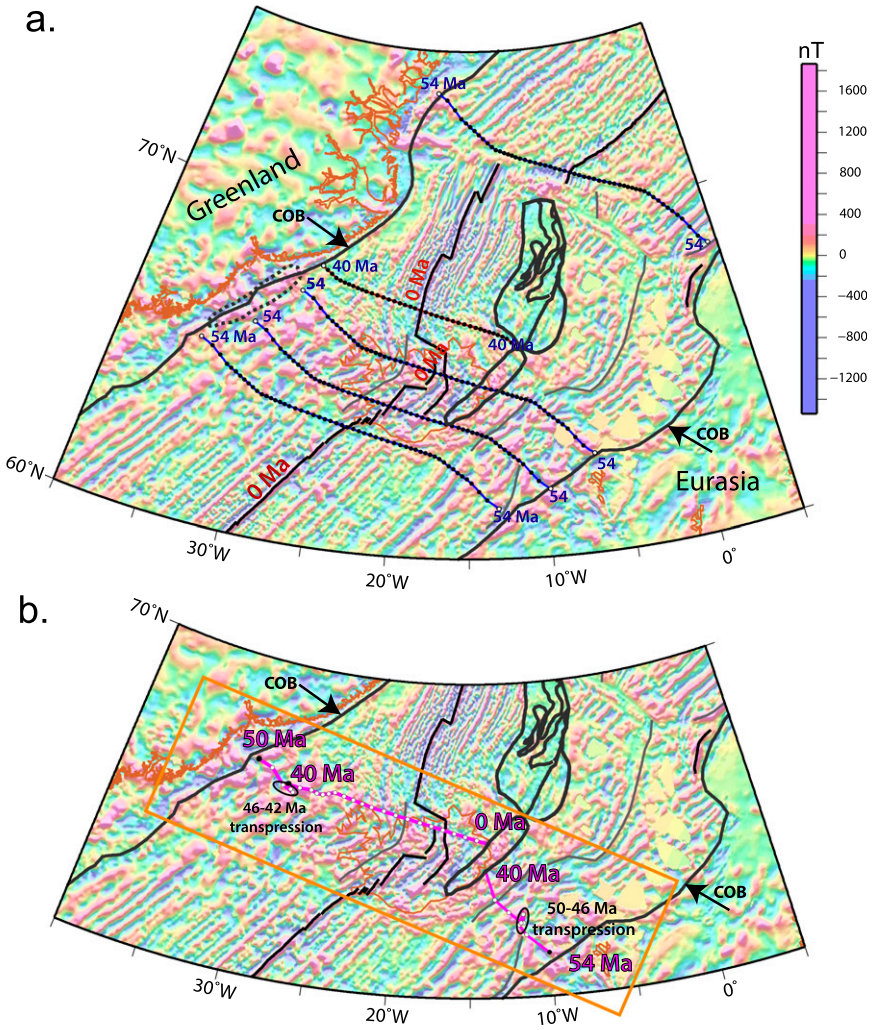

Fig. S2. (*A*) Flow lines showing the direction and amount of (symmetric) seafloor spreading between Eurasia and Greenland and between Greenland and JMM calculated in 2-My time intervals from stage poles derived from the Gaina et al. (1) kinematic model. That model was derived from magnetic anomalies identified north and south of Iceland. The base map shows the total magnetic anomaly grid of the northeast Atlantic (2). Thin dark gray lines represent the identified continent–ocean boundaries (COBs). Note the position and extent of JMM-E (dashed line) next to the Greenland COB in a reconstructed (54 Ma) position. (*B*) Motion path of JMM-E relative to Eurasia (magenta lines east of JMM-E) and of the JMM-E relative to Greenland (magenta lines west of JMM-E) in 2-My intervals. Due to competing midocean-ridge propagation from northeast (the Ægir Ridge) and from southwest (the Reykjanes ridge) between 50 and 42 Ma, JMM-E experienced rotation, and its boundaries with surrounding continental and oceanic crust were subjected to transpression and strike–slip motion (see motion path segments within the black ellipses). This time interval coincided with major reorganizations in the northeast Atlantic suggested by changes in seafloor spreading directions and rates (1, 3). Due to these tectonic events and magmatic overprint from the Iceland plume, the magnetic anomaly data show a quasichaotic pattern across the Iceland-Faroe ridge (orange rectangle).

1. Gaina C, Gernigon L, Ball P (2009) Palaeocene—Recent plate boundaries in the NE Atlantic and the formation of the Jan Mayen microcontinent. *J Geol Soc London* 166:601–616.
2. Gaina C, Werner S, Saltus R, Maus S, CAMP-GM Group (2011) Circum-Arctic Mapping Project: New magnetic and gravity anomaly maps of the Arctic. *Arctic Petroleum Geology*, eds Spencer AM, Embry AF, Gautier DL, Stoupakova AV, Sørensen K, Geological Society London, Memoirs (Geological Society, London), Vol 35, pp 39–48.
3. Gernigon L, et al. (2012) The Norway Basin revisited: From continental breakup to spreading ridge extinction. *Mar Pet Geol* 35:1–19.

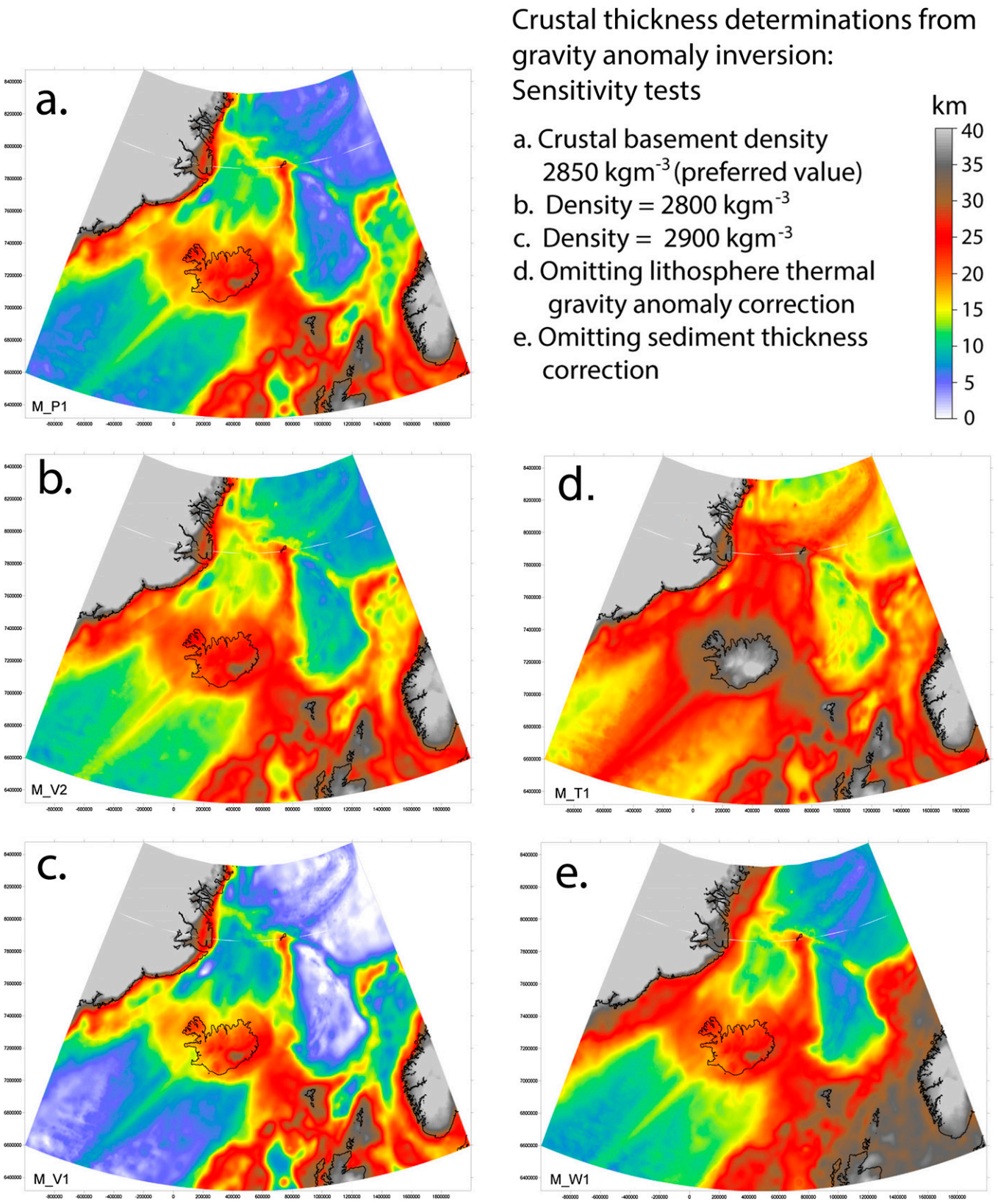

Fig. S3. Crustal thickness maps derived from gravity anomaly inversion (detailed in refs. 1–3) showing sensitivity to crustal basement density, lithosphere thermal gravity anomaly correction, and sediment thickness correction. (*A*) Crustal basement density, 2,850 kg·m^{-3} (preferred value, as in Fig. 1). (*B*) Crustal basement density, 2,800 kg·m^{-3}. (*C*) Crustal basement density, 2,900 kg·m^{-3}. (*D*) Omitting a lithosphere thermal gravity anomaly correction results in the prediction of a Moho that is too deep and a crustal thickness that is too large (1). The lithosphere thermal gravity anomaly correction is calculated using a 3D lithosphere thermal model incorporating the spatial variation in the initial lithosphere thermal perturbation and thermal reequilibration (i.e., cooling) time.

Legend continued on following page

The lithosphere thermal perturbation for breakup and seafloor spreading is defined using the lithosphere thinning factors ($1 - 1/\beta$) and the model of McKenzie (4). For continental lithosphere, this thinning factor is derived from the gravity inversion; for oceanic lithosphere, it may also be derived from the gravity inversion or alternatively may be set to 1 (corresponding to β = infinity), where a priori reliable ocean isochron data exist (Fig. 8*B*). For continental margin lithosphere, the cooling time is breakup age; for oceanic lithosphere, the cooling time is the ocean isochron age. Errors in ocean isochron location and age cause errors in the lithosphere thermal gravity anomaly correction and as a consequence the Moho depth, crustal thickness, and lithosphere thinning derived from gravity inversion. Therefore, the oldest isochrons adjacent to the continent–ocean boundary are not usually used in the gravity inversion; in this study, a continental breakup age of 55 Ma is assumed for the northeast Atlantic and the oldest ocean isochron used is 50 Ma (about chron 22 time in Fig. 8*A*). Sensitivity tests have also been carried out to the use of isochrons to condition the 3D lithosphere thermal model used to calculate the lithosphere thermal gravity anomaly correction incorporated in the gravity inversion. These tests show that the predicted thicker crust under JMM and southeast Iceland are not significantly dependent on ocean-age isochrons used to determine the lithosphere thermal gravity anomaly correction, and that the thicker crust under the JMM, compared with that of the oceanic basins to the east and west, extends southwestward into southeast Iceland. (*E*) Omitting the sediment thickness gravity anomaly contribution from the gravity inversion (or using too small sediment thickness) leads to an overestimate of Moho depth and crustal basement thickness. The sediment thickness grid used in this study is a merge of the Divins (5) and Laske et al. (6) compilations, and sediment density used in the gravity inversion assumes a compaction-controlled density–depth relationship. The same reference Moho depth of 35 km is used for gravity inversion solutions *A*, *B*, and *C*.

1. Chappell AR, Kusznir NJ (2008) Three-dimensional gravity inversion for Moho depth at rifted continental margins incorporating a lithosphere thermal gravity anomaly correction. *Geophys J Int* 174:1–13.
2. Greenhalgh EE, Kusznir NJ (2007) Evidence for thin oceanic crust on the extinct Aegir Ridge, Norwegian Basin, NE Atlantic derived from satellite gravity inversion. *Geophys Res Lett* 34(6):L06305.
3. Alvey A, Gaina C, Kusznir NJ, Torsvik TH (2008) Integrated crustal thickness mapping and plate reconstructions for the High Arctic. *Earth Planet Sci Lett* 274:310–321.
4. McKenzie D (1978) Some remarks on the development of sedimentary basins. *Earth Planet Sci Lett* 40:25.
5. Divins DL (2008) Total sediment thickness of the World's oceans and marginal seas. NGDC. Available at https://www.ngdc.noaa.gov/mgg/sedthick/sedthick.htm. Accessed May 21, 2014.
6. Laske G, Masters G (1997) A global digital map of sediment thickness. *Eos Trans AGU* 78:F483.

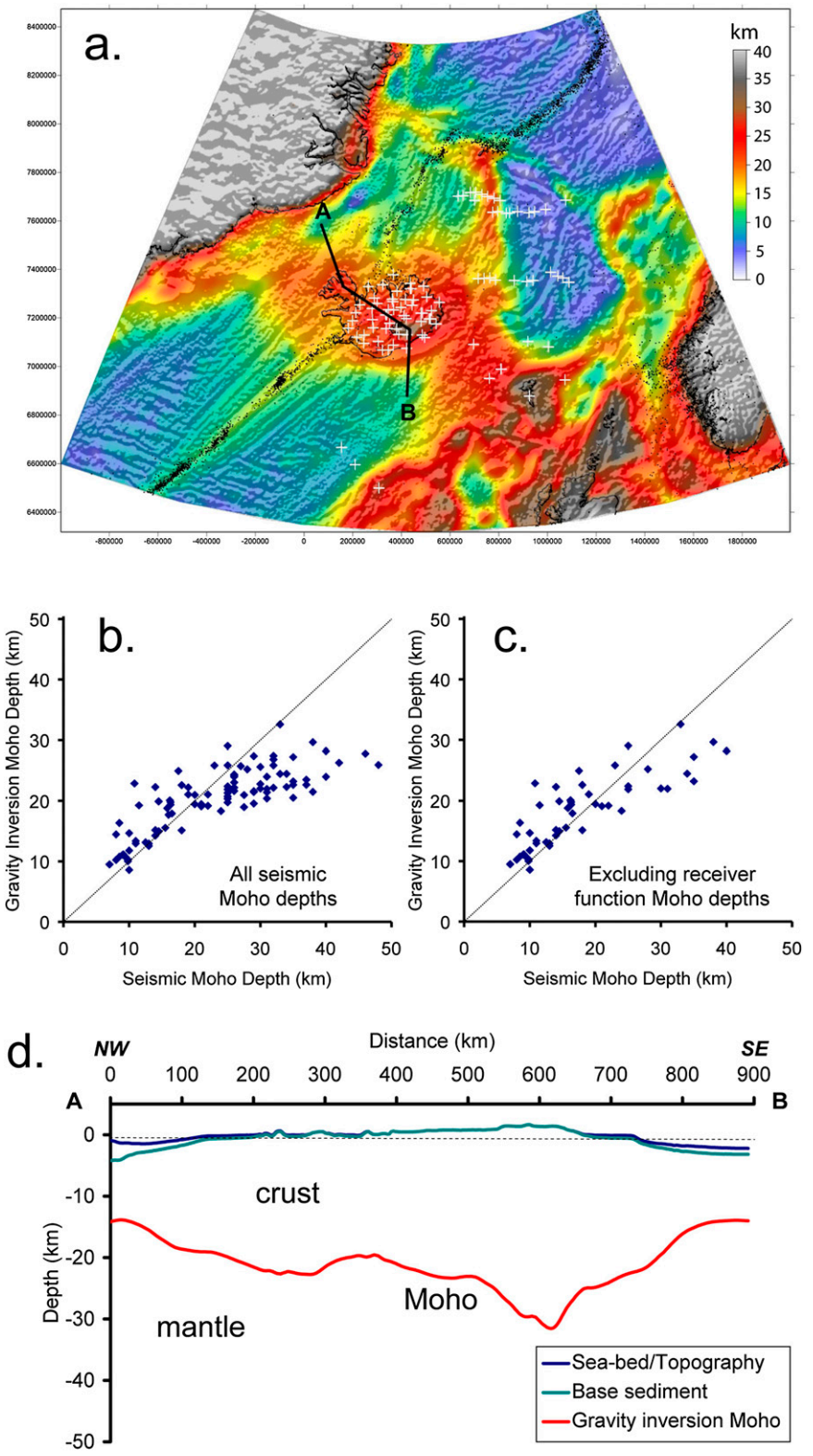

Fig. S4. (*A*) Location of seismically determined Moho depth measurements (white +) for comparison with Moho depths determined from gravity inversion (as in Fig. 1). (*B*) Cross-plot of gravity versus seismically (1–16) determined Moho depths. (*C*) Cross-plot excluding seismically determined Moho depth using receiver function analysis. Cross-plots show a good correlation, but at larger Moho depths, seismic values are consistently greater than gravity-determined values, suggesting that the gravity inversion may be underestimating Moho depths. One explanation for this may be that that the densities of thicker (or deeper) crust may be larger than the preferred value of 2,850 kg·m^{-3} used in the gravity inversion. Some of the seismic Moho depth determinations are large, exceeding 40 km; some of these large values correspond to receiver function determinations that may be overestimating Moho depth. (*D*) Crustal cross-section A–B with

Legend continued on following page

Moho depth determined using gravity inversion. The crustal cross-section—running from the northern Denmark Strait across Iceland from Snæfellnes to Öræfajökull and then into the northeast Iceland Basin—shows thickest crust under southeast Iceland.

1. Darbyshire FA, White RS, Priestley KF (2000) Structure of the crust and uppermost mantle of Iceland from a combined seismic and gravity study. *Earth Planet Sci Lett* 181:409–428.
2. Darbyshire FA, et al. (2000) Crustal structure of central and northern Iceland from analysis of teleseismic receiver functions. *Geophys J Int* 143:163–184.
3. Kumar P, Kind R, Priestley K, Dahl-Jensen T (2007) Crustal structure of Iceland and Greenland from receiver function studies. *J Geophys Res* 112(B3):B03301.
4. Foulger GR (2006) Older crust underlies Iceland. *Geophys J Int* 165:672–676.
5. Breivik AJ, Mjelde R, Faleide JI, Murai YJ (2006) Rates of continental breakup magmatism and seafloor spreading in the Norway Basin-Iceland plume interaction. *J Geophys Res* 111(B7): B07102.
6. Breivik AJ, Mjelde R, Faleide JI (2008) Neogene magmatism northeast of the Aegir and Kolbeinsey ridges, NE Atlantic: Spreading ridge mantle plume interaction? *Geochem Geophys Geosyst* 9(2):Q02004.
7. Breivik AJ, Mjelde R, Faleide JI, Muro Y (2012) The eastern Jan Mayen microcontinent volcanic margin. *Geophys J Int* 188:798–818.
8. Bohnhoff M, Makris J (2004) Crustal structure of the southeastern Iceland-Faeroe Ridge (IFR) from wide aperture seismic data. *J Geodyn* 37:233–252.
9. Harland KE, White RS, Soosalu H (2009) Crustal structure beneath the Faroe Islands from teleseismic receiver functions. *Geophys J Int* 177:115–124.
10. Kodeira S, Mjelde R, Gunnarsson K, Shiobara H, Shimamura H (1998) Structure of the Jan Mayen microcontinent and implication for its evolution. *Geophys J Int* 132:383–400.
11. Kodeira S, Mjelde R, Shiobara H, Shimamura H (2002) Evolution of oceanic crust on the Kolbeinsey Ridge, north of Iceland, over the past 22 Myr. *Terra Nova* 10(1):27–31.
12. Mjelde R, et al. (2008) Magmatic and tectonic evolution of the North Atlantic. *J Geol Soc Lond* 165:31–42.
13. Mjelde R, Aurvåg R, Kodaira S, Shimamura H, Gunnarsson K (2002) Vp/Vs-ratios from the central Kolbeinsey ridge to the Jan Mayen basin, North Atlantic; implications for lithology, porosity and present-day stress field. *Mar Geophys Res* 23:125–145.
14. Richardson KR, Smallwood JR, White RS, Snyder DB, Maguire PKH (1998) Crustal structure beneath the Faroe Islands and the Faroe–Iceland Ridge. *Tectonophysics* 300:159–180.
15. White RS, et al. (2008) Lower-crustal intrusion on the North Atlantic continental margin. *Nature* 452(7186):460–464.
16. White RS, Smith LK (2009) Crustal structure of the Hatton and the conjugate east Greenland rifted volcanic continental margins, NE Atlantic. *J Geophys Res* 114(B2):B02305.

Table S1. Absolute reconstruction parameters (Euler poles) for the Cenozoic

Age, Ma	Continent, microcontinent	Latitude, °	Longitude, °	Angle, °
27	Greenland (as North America)	51.3	131.8	5.5
	All Jan Mayen Blocks and Eurasia	58.7	316.6	−2
33	Greenland	53.8	125	6.6
	Jan Mayen/Jan Mayen South*	65.5	337.7	−12.3
	Jan Mayen Extended	52.8	40.8	2.4
	Eurasia	59.1	293.6	−2.1
40	Greenland	44.5	114.9	7.5
	Jan Mayen	55.3	310.4	−8
	Jan Mayen South*	65.6	326	−16.6
	Jan Mayen Extended	18	253.9	−2.6
	Eurasia	50.3	264.6	−2.7
45	Greenland	47.2	107.8	7.8
	Jan Mayen	58.3	309.3	−9.6
	Jan Mayen South*	66.3	324.3	−18.2
	Jan Mayen Extended	47.8	31	6.5
	Eurasia	42.4	224.5	−2.5
52	Greenland	45.6	98.1	9.2
	Jan Mayen	61.2	313.7	−15.7
	Jan Mayen South*	65.9	324.3	−24.3
	Jan Mayen Extended	53.5	264.5	−6.1
	Eurasia	27.7	200.6	−3.4
55†	Greenland	46.9	101.6	8.8
	Jan Mayen	62.9	321.5	−18.3
	Jan Mayen South*	66.4	329.5	−27
	Jan Mayen Extended	21	240	−3.6
	Eurasia	30.9	208.2	−2.9
60†	Greenland	47.1	89.7	9.3
	Jan Mayen	62.7	308.4	−16
	Jan Mayen South*	67.5	320.3	−24.7
	Jan Mayen Extended	65.1	286.3	−11.1
	Eurasia	29.6	178.7	−5.2

*The Jan Mayen Microcontinent block marked S in Fig. 8*B*.
†Reconstructions at 55 and 60 Ma include minor prebreakup extension. Estimated prebreakup extension for Eurasia relative Greenland based on Gaina et al. (1).

1. Gaina C, Roest WR, Muller RD (2002) Late Cretaceous-Cenozoic deformation of northeast Asia. *Earth Planet Sci Lett* 197:273–286.

Table S2. Euler poles for relative motion versus a fixed Greenland

Age, Ma	Continent, microcontinent	Latitude, °	Longitude, °	Angle, °
27	All Jan Mayen Blocks and Eurasia	68.5	131.9	−6.5
33	Jan Mayen/Jan Mayen South*	82.3	20.8	−16.7
	Jan Mayen Extended	39.3	145.3	−5.2
	Eurasia	68.2	131.5	−7.6
40	Jan Mayen	84.6	75.8	−11.9
	Jan Mayen South*	82.6	9.2	−20.7
	Jan Mayen Extended	56.6	141.6	−7.2
	Eurasia	60.0	129.5	−8.3
45	Jan Mayen	84.5	40.4	−14.1
	Jan Mayen South*	81.5	3.6	−22.9
	Jan Mayen Extended	6.9	149.7	−6.2
	Eurasia	56.3	128.9	−8.9
52	Jan Mayen	80.9	8.3	−20.7
	Jan Mayen South*	79.1	358.4	−29.6
	Jan Mayen Extended	74.2	122.4	−11.9
	Eurasia	50.0	125.1	−10.4
55†	Jan Mayen	80.7	4.1	−21.5
	Jan Mayen South*	79	356.9	−30.4
	Jan Mayen Extended	83.9	73.2	−17
	Eurasia	52.4	123.5	−12.0
60†	Jan Mayen	80.7	4.1	−21.52
	Jan Mayen South*	79.2	357.6	−30.4
	Jan Mayen Extended	83.9	73.2	−17
	Eurasia	48.3	124.5	−12.2

*The Jan Mayen Microcontinent block marked S in Fig. 8*B*.
†Reconstructions at 55 and 60 Ma include minor prebreakup extension. Estimated prebreakup extension for Eurasia relative Greenland based on Gaina et al. (1).

1. Gaina C, Roest WR, Muller RD (2002) Late Cretaceous-Cenozoic deformation of northeast Asia. *Earth Planet Sci Lett* 197:273–286.

Other Supporting Information Files

Dataset S1 (XLSX)